MATHEMATICAL BIOSCIENCES
AND ENGINEERING
Volume **2**, Number **2**, April **2005**

http://www.mbejournal.org/

pp. **381–418**

THE ECOLOGY AND EVOLUTIONARY BIOLOGY OF CANCER: A REVIEW OF MATHEMATICAL MODELS OF NECROSIS AND TUMOR CELL DIVERSITY

John D. Nagy

Department of Life Sciences, Scottsdale Community College
9000 E. Chaparral Rd., Scottsdale, AZ 85256

School of Life Sciences, Arizona State University
PO Box 874501, Tempe AZ, 85287-4501

(Communicated by Yang Kuang)

Abstract. Recent evidence elucidating the relationship between parenchyma cells and otherwise "healthy" cells in malignant neoplasms is forcing cancer biologists to expand beyond the genome-centered, "one-renegade-cell" theory of cancer. As it becomes more and more clear that malignant transformation is context dependent, the usefulness of an evolutionary ecology-based theory of malignant neoplasia becomes increasingly clear. This review attempts to synthesize various theoretical structures built by mathematical oncologists into potential explanations of necrosis and cellular diversity, including both total cell diversity within a tumor and cellular pleomorphism within the parenchyma. The role of natural selection in necrosis and pleomorphism is also examined. The major hypotheses suggested as explanations of these phenomena are outlined in the conclusions section of this review. In every case, mathematical oncologists have built potentially valuable models that yield insight into the causes of necrosis, cell diversity, and nearly every other aspect of malignancy; most make predictions ultimately testable in the lab or clinic. Unfortunately, these advances have gone largely unexploited by the empirical community. Possible reasons why are considered.

1. **Introduction.** Modern cancer theory is founded on two central questions. First, how do malignant tumors arise from previously healthy, genomically intact cells? Second, why do malignant tumors tend to share similar characteristic behaviors—uncontrolled growth, lack of tissue integration, invasion of surrounding tissue, and metastasis? Although neither question has been answered satisfactorily in detail, over the past twenty years researchers have established at least the broad outlines of the answers, primarily because of advances in molecular biology. As a natural consequence, we describe cancer etiology in terms of genetic and epigenetic changes in key genes scattered throughout the genome [35, 50, 51, 70, 95]. Here the phrase "genetic changes" is understood to mean mutations, and in this context "epigenetic changes" usually refers to methylation or acetylation of DNA or chromatin-associated histones [95, 111] that can alter gene transcription patterns. Such genomic alterations in humans are commonly caused by environmental factors

2000 *Mathematics Subject Classification.* 92-02.

Key words and phrases. cancer, mathematical models, necrosis, pleomorphism, genetic polymorphism, natural selection, review.

(see [116] for a recent review) that either directly damage DNA (mutagens), such as coal tars in cigarette smoke or UV radiation, or cause irritation and subsequent cell turnover in tissues (mitogens), for example, asbestos or inhaled particulates in cigarette smoke or pollution. Viruses can also cause oncogenic changes in cells, either by inserting an oncogene or oncoprotein directly into a cell or by disrupting gene regulation as the viral genome is integrated into the host's DNA.

Since most cancer theory revolves around "key genes" and their products, most basic cancer research attempts to identify the location of these genes, their normal function, and how their structural and functional disruption leads to cancer. Perhaps the most complete and lucid statement of modern cancer theory, what I will refer to as the standard theory, was presented by Douglas Hanahan and Robert Weinberg in 2000 [51]. In short, the standard theory suggests that transformation occurs if and only if a single cell acquires the following six characteristics: (1) self-stimulated proliferation; (2) unresponsiveness to external inhibitory signals; (3) malfunction of apoptotic machinery; (4) ability to promote tumor angiogenesis; (5) immortalization; and (6) ability to invade surrounding tissue and metastasize. Acquisition of each attribute represents a step toward malignancy, and cells in intermediate steps can be recognized as benign, sometimes premalignant lesions [112]. I should note that Hanahan and Weinberg do not press the theory quite this far; rather, they seem to suggest that these conditions are *usually* necessary and perhaps not always sufficient. Such is the complexity of this disease.

On its face, the standard theory attempts to answer only one question—what causes malignant tumors? However, the conventional focus on genomics of a single transformed cell suggests that the second foundational question—why do cancers behave as they do—is answered as a mere corollary. Since cancers arise from "one renegade cell" [113] and the genomes of this cell's clones ultimately govern tumor behavior, knowing the function of the altered genes should explain that behavior. For example, we recognize that inactivating mutations in the tumor suppressor gene *p53* propel a cell partway down the path toward malignancy. If that cell becomes cancerous, its loss of *p53* explains at least one of its characteristic behaviors—evasion of apoptosis.

2. **Inadequacies of the standard theory.** Although this "genome-centered" theory dominates the field [20, 36], its adequacy is not universally accepted [32, 36, 58, 67]. The critics, while rarely disputing the importance of cancer cell genomics, recognize that cancer is not the manifestation of "a transformed cell." Rather, it arises by natural selection acting on a variety of multiply mutated cells in the context of the host's physiology, resulting in disrupted tissue architecture and loss of tissue homeostasis. Therefore, any accurate theory must include interactions among a variety of genetically distinct parenchyma (cancer) cell types, perhaps genetically altered stromal cells, and unmutated healthy cells, both peritumoral and distant. Although these interactions certainly are influenced by genomes, the genomes of a variety of cell types, both cancerous and healthy, are involved. Also, knowledge of genomes alone cannot predict in any practical way a tumor's clinical behavior, because the interactions among cell types are far too complicated. Therefore, genome-centered research may not be as fruitful as originally hoped, and certainly theorists must recognize that tumor behavior is at least as much an ecological and evolutionary problem as a molecular one.

The empirical basis for shifting focus from the one-renegade-cell concept to the ecosystem concept comes from numerous observations that the standard theory has difficulty explaining. For example, substantial evidence exists that fibroblasts, normal denizens of extracellular matrix (ECM) in both healthy and tumor tissue, in part control whether a carcinoma develops and its subsequent behavior (reviewed in [17]). For example, fibroblasts from a malignant prostate tumor cocultured with epithelial cells from a benign prostate tumor promote malignant transformation of the benign cells. Normal fibroblasts do not, nor do tumor fibroblasts cocultured with normal epithelial cells [53, 86]. Further evidence comes from a study in which breast epithelial cells were transplanted into irradiated and nonirradiated mammary fat pads in live mice [12]. Breast malignancies of epithelial origin arose in about 80% of irradiated fat pads, compared to only about 20% of controls, and tended to be more aggressive in mice with irradiated fat pads. Prior to irradiation and transplantation, native epithelial cells had been removed, so these tumors arose from the injected, untransformed epithelial cells. The authors conclude that radiation damage to native fibroblasts of host mice promotes tumorigenesis of epithelial cells. These observations are corroborated by microdissection studies of the stroma in human breast and colon cancers in which stromal cells showed genetic abberations—loss of heterozygosity, microsatellite instability, and mutations in *p53*—that are also characteristic of cancer cells [115]. It appears, then, that genetic alterations in stromal fibroblasts in addition to genomic changes in the renegade cells are important events on the road to cancer.

More recent research supports this conclusion. Kenoki Ohuchida et al. [85], for example, found that pancreatic cancer cells tended to be more invasive, at least in an in vitro invasion assay, when cocultured with irradiated versus nonirradiated fibroblasts. Certain other manipulations lead the authors to conclude that irradiated fibroblasts secrete a soluble chemical signal enhancing invasive activity of the cancer cells. No matter the cause, malignant transformation apparently depends not just on one cell type's genetic status but also on the behavior of untransformed cells in its ecosystem.

Another problem with the one-renegade-cell theory is its prediction that tumors should be monoclonal. However, "evidence is now accruing, at least for a subset of epithelial tumors, that by no means all of these lesions are [mono]clonal, with the result that we probably have to come to terms with the concept that tumorigenesis in epithelial systems demands the co-operation of several distinct clones, and somehow account for this in any global theory of carcinogenesis" [20, p.90]. Even for tumors that are inarguably monoclonal, the standard theory itself posits that the single, fully malignant cell arises because natural selection favors it in the competition with other altered cells in premalignant lesions. This view is so well accepted that it can be found in most standard textbooks (for example, see the cancer and neoplasia chapters in [5] and [28]). So, natural selection and tumor ecology should play central roles in cancer theory.

Although cancer theory derived from molecular and cellular biology largely ignores evolutionary and ecological relationships, the same cannot be said for theory developed by mathematical biologists, who for the last thirty years have produced an enormous variety of mathematical models of malignant neoplasia. These models rely heavily on formalisms previously applied to ecology but adapted almost directly to tumor ecosystems—Gompertz and logistic models to represent tumor cell population dynamics, Lotka-Volterra models of competition among cells for

nutrients, von Förster–like forms for age-structured population models, and more general reaction-diffusion models for spatially explicit competition, to name a few. The theory growing from these modeling efforts is the focus of this review.

Mathematical oncologists must constantly revisit the relevance of existing mathematical models of tumor ecology to modern cancer biology and what needs to happen to complete the ecology-based theory and facilitate its entry into mainstream oncology. Although these questions sparked this review, they are unfortunately far too broad for a single article to span. Instead I adopt the more modest goal of reviewing how an evolutionary-ecology outlook has helped theoretical oncologists develop hypotheses to explain two common characteristics of malignant neoplasia—necrosis and tumor cell diversity. In section 3, I focus on necrosis, starting with a description of a tissue culture model of malignant neoplasia, called the multicell spheroid, famous within the mathematical oncology community (section 3.1). Then I examine models of necrosis caused by nutrient limitation (section 3.2), mechanical disruption of cells (section 3.3), local acidosis (section 3.4), and finally local ischemia (section 3.5). In section 4, I discuss the issue of cell diversity within tumors, including diversity among all cell types (section 4.1) and pleomorphism among parenchyma cells (section 4.2). In section 5, I then examine models that show the interrelation between the causes of pleomorphism and necrosis. Finally, in section 6 I summarize this body of research and ask, if no mathematical models of cancer had ever been constructed, how would our understanding of necrosis and tumor cell diversity be different?

3. **Necrosis: What causes the tumor ecosystem to collapse?**

Malignant tumors in vivo and certain tissue models variously called multicell spheroids, tumor spheroids or avascular spheroids, typically are characterized by regions of necrosis (Fig. 1). Although it might seem obvious that these necrotic zones arise through "lack of nutrient," various more detailed hypotheses have been presented in the mathematical and theoretical literature. Possible immediate causes include deficiencies in oxygen, glucose, or perhaps other nutrients, such as phosphorus [34, 60] or iron [30, 52, 63, 91]. Some researchers suggest that inhibitory chemicals, which could be metabolic waste or other compounds, might play a role. Still others implicate mechanical destruction of cells. At one level removed from the immediate cause, if nutrient deficiency, toxin production, or both are to blame, local ischemia is almost certainly involved. But then what causes the ischemia—inefficient neoangiogenesis (the tumor "outgrowing" its blood supply), blood vessel collapse, variation in hematocrit distribution in a microvascular net, or some combination of the three? All of these hypotheses have been the subjects of mathematical investigations, which I review in the following subsections.

3.1. **Necrosis in multicell spheroids.**

Multicell spheroids have enjoyed considerable attention from mathematical oncologists, probably more than any other tissue model of malignancy. Studied both empirically and theoretically for more than thirty years [48, 105], multicell spheroids "are of intermediate complexity [as tissue models of cancer] between *in vitro* monolayers and tumors *in vivo*" [104, p.1669] (see also [61]). One can grow them either in suspension or in a gel by inducing a clump of transformed cells to proliferate into a stable, somewhat symmetrical ball of cells usually no more than 2 mm in diameter (see [78, 104] for pictures of spheroids). Sectioning a larger spheroid through its equator can reveal at least two, sometimes three or more, histologically or physiologically distinct regions. Most

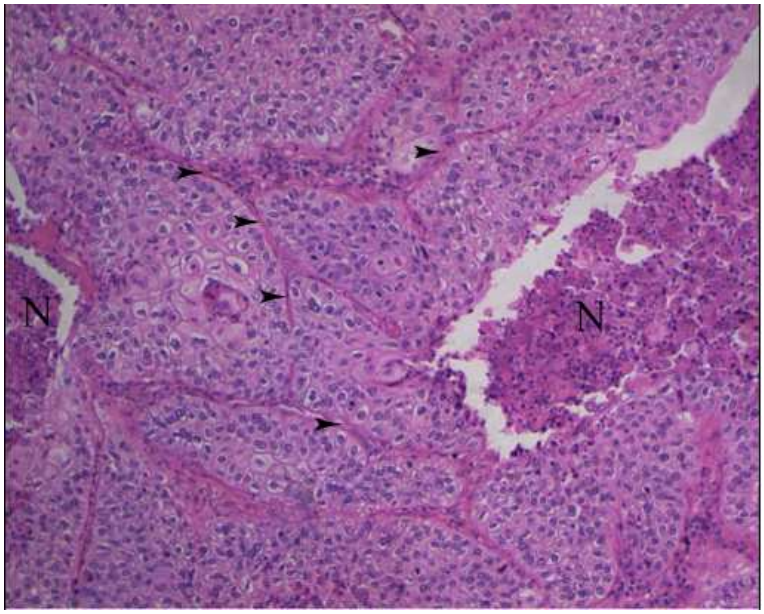

FIGURE 1. Squamous cell lung cancer, H. & E. stain, 100× original magnification. Regions labelled "N" are necrotic, and arrows point to examples of ECM. Purple dots in the necrotic regions are mostly immune cell nuclei, primarily of neutrophils. Note how cancer cells form deranged sheets reminiscent of epithelium but with a highly disturbed architecture.

commonly one finds a core of necrotic tissue surrounded by a layer of living cells up to about 150 μm thick. Typically, this annulus of living cells has an exterior rind of proliferative tissue. Beneath this rind, between it and the necrotic core, often exists a layer of "quiescent" cells—alive but not dividing (Fig. 2).

The obvious hypothesis explaining this characteristic histological pattern—that cells in the interior die or stop reproducing because they suffer a profound lack of nutrient caused by diffusion limitation and competition—is compelling but probably too simple [77, 78]. Either from a recognition of the true complexity or pure luck, the obvious hypothesis was almost instantly discarded by mathematical modelers in favor of more complicated mechanisms. The influential series of papers by H. P. Greenspan [48, 49], published in the early 1970s but motivated by earlier models [21, 110], stands as an example. In these models, Greenspan included a hypothesized inhibitory chemical, produced either by necrotic tissue or living cells, that along with nutrient deficiency explained the observed pattern of necrosis in multicell spheroids. These papers were among the first to present mechanistic explanations of tumor behavior, as opposed to contemporary studies assuming a Gompertzian phenomenonology (reviewed in [10]), and spawned an enormous number of subsequent models (reviewed in [1, 10, 22]).

Because it forms part of the foundation of mathematical oncology, a quick survey of Greenspan's approach helps us understand subsequent developments. In this study [48], Greenspan assumes the simplest possible geometry for the spheroid—an actual perfect sphere of radius $R_0(t)$ at time t. (Here, as elsewhere, I attempt to

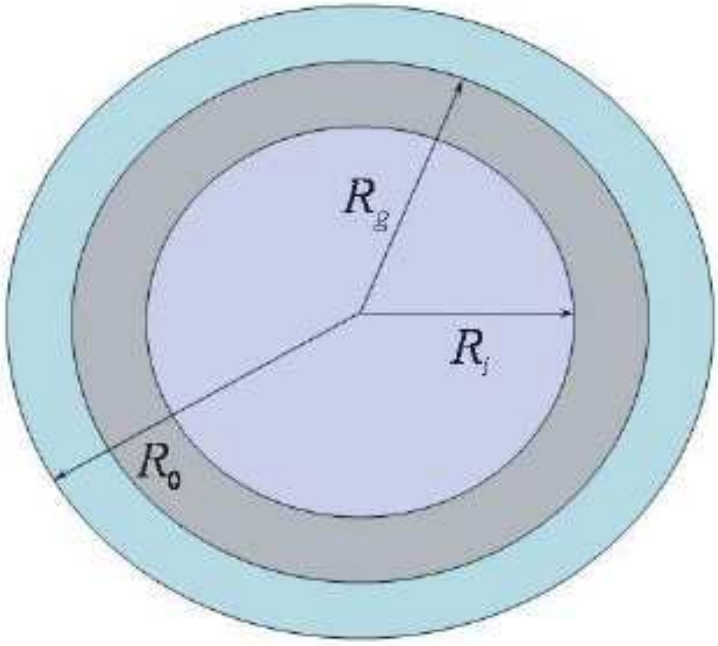

FIGURE 2. Idealized cross section through a multicell spheroid. The necrotic core has radius R_i; the annulus of quiescent cells has outer radius R_g, and the spheroid itself has radius R_0. Based on Fig. 1 in [48, p.318].

preserve the author's original notation unless simplification clarifies the presentation.) The spherical shape is maintained by surface tension and incompressibility of cells and necrotic debris. Cell kinetics depend on two diffusible compounds: a nutrient like oxygen or glucose, with concentration $\sigma(r)$, supplied by the media, and a toxin produced within the spheroid, with concentration denoted $\beta(r)$, where r represents radial position within the spheroid.

Greenspan hypothesizes that lack of nutrient drives necrosis; the inhibitor simply modifies the cell proliferation rate. Therefore, he assumes a minimum nutrient concentration σ_l below which cells die. Therefore, the center of the spheroid may contain a necrotic core of radius $R_i(t)$ if $\sigma(r) < \sigma_l$ for $0 \leq r \leq R_i$. Greenspan further hypothesizes that quiescence arises from the inhibitor, not lack of nutrient. He initially leaves the source of the toxin incompletely specified and then builds two models—one in which the toxin is released by disintegrating necrotic cells (see equation (1)), and the other assuming the toxin is metabolic waste or some other secretion from living cells (see (3)). In any event, if the inhibitor concentration rises above some threshold β_l, mitosis in cancer cells ceases. Therefore, in addition to a necrotic core, a "core of quiescence" of radius R_g can also develop if $\beta(r) > \beta_l$ for $0 \leq r \leq R_g$. The often-observed histology of a necrotic core surrounded by an annulus of quiescent tissue further surrounded by a rind of proliferative tissue will develop if the nutrient and inhibitor profiles allow $R_i < R_g < R_0$ (Fig. 2).

Both the nutrient and putative toxin are assumed to diffuse on a much shorter time scale than cell proliferation, so Greenspan passes to the quasi-steady-state

approximation under the assumption of diffusive equilibrium. With these primary assumptions, among others, Greenspan arrives at the following model in spherical coordinates:

$$\begin{cases} R_0^2 \dfrac{\mathrm{d}R_0}{\mathrm{d}t} &= \dfrac{s}{3}[R_0^3 - \max(R_i^3, R_g^3)] - \lambda R_i^3, \\ \dfrac{1}{r^2}\dfrac{\partial}{\partial r}\left(r^2 \dfrac{\partial}{\partial r}\sigma(r,t)\right) &= \dfrac{A}{k} H(r - R_i) H(R_0 - r), \\ \dfrac{1}{r^2}\dfrac{\partial}{\partial r}\left(r^2 \dfrac{\partial}{\partial r}\beta(r,t)\right) &= -\dfrac{P}{\kappa} H(R_i - r), \end{cases} \tag{1}$$

with s the constant per unit proliferation rate in the proliferative rind, λ the rate at which necrotic cells disintegrate, k and κ the respective diffusion constants for nutrient and toxin, A the constant rate at which living cells consume nutrient, P the constant per-unit production rate of toxin from the necrotic core, and $H(\cdot)$ the Heaviside step function:

$$H(a) = \begin{cases} 1 & ; \quad a \geq 0, \\ 0 & ; \quad a < 0. \end{cases} \tag{2}$$

If instead of emanating from the necrotic core the toxin's source is assumed to be living cells, then the right-hand side of the third equation in model (1) becomes

$$-\frac{P}{\kappa} H(R_0 - r) H(r - R_i). \tag{3}$$

Greenspan's models suggested a very simple experiment to test the inhibitor's effect, if any, on spheroid dynamics. In short and ignoring certain technical details, one would grow spheroids under standard conditions allowing reproducible behavior, begin sectioning samples of spheroids just before and after they enter the first growth retardation phase, and measure the extent of necrosis. From such measurements one can obtain quantitative estimates of the inhibitor's impact over time in terms of the proportion of cells reproducing. Of course, this model's assumption that cells either reproduce at a constant rate or not at all is almost certainly unrealistic; however, the result still has meaning as a measure of the inhibitor's impact. In the simplest case, this procedure can at least establish whether the inhibitor exists. Apparently, however, these models failed to impress the empirical community and were never used to determine the role of an inhibitor in necrosis development [10].

3.2. **Necrosis caused by diffusion-limited nutrient delivery.** Greenspan's results did impress theorists, sparking an avalanche of research that is not yet spent. Part of this avalanche used Greenspan's model as a basis to refine the diffusion-limitation hypothesis, which I briefly review next. Parallel with these studies, another formalism developed that also was used to probe diffusion limitation. This set of models focuses on tumor cords, essentially spheroids turned inside-out. Below I outline some of the main results from both types of models.

3.2.1. *Diffusion limitation in multicell spheroids.* Among the more influential research threads using multicell spheroids to study necrosis is a series of papers by Helen Byrne and Mark Chaplain [23, 24]. These models represent a small spheroid, which Byrne and Chaplain interpret as a tiny in vivo tumor. The first of these models [23] assumes that no necrotic core exists and takes the following form under

the quasi-steady-state approximation of diffusive equilibrium for both the nutrient and inhibitor:

$$\begin{cases} R^2 \dfrac{\mathrm{d}R}{\mathrm{d}t} &= \displaystyle\int_0^{R(t)} S(\sigma,\beta) r^2 \,\mathrm{d}r, \\ 0 &= \dfrac{D_1}{r^2}\dfrac{\partial}{\partial r}\left(r^2 \dfrac{\partial \sigma}{\partial r}\right) + \Gamma(\sigma_B - \sigma) - \lambda\sigma - g_1(\sigma,\beta), \\ 0 &= \dfrac{D_2}{r^2}\dfrac{\partial}{\partial r}\left(r^2 \dfrac{\partial \beta}{\partial r}\right) - g_2(\sigma,\beta), \end{cases} \tag{4}$$

with the following notation: R is the radius of the spheroid; $S(\sigma,\beta)$ is cell proliferation rate; D_1 and D_2 are diffusivities of nutrient and inhibitor, respectively; Γ measures vascular delivery of nutrient; σ_B is concentration of nutrient in the blood plasma; g_1 and g_2 represent sources and sinks of nutrient and inhibitor, respectively, within the spheroid; and all other notation is consistent with model (1). They subsequently [24] apply Greenspan's original hypothesis that necrosis occurs whenever the nutrient concentration falls below some critical value to obtain this model:

$$\begin{cases} R^2 \dfrac{\mathrm{d}R}{\mathrm{d}t} &= \displaystyle\int_0^{R(t)} [S(\sigma,\beta)H(r-r_i) - N(\sigma,\beta)H(r_i - r)] r^2 \,\mathrm{d}r, \\ 0 &= \dfrac{D_1}{r^2}\dfrac{\partial}{\partial r}\left(r^2 \dfrac{\partial \sigma}{\partial r}\right) - [\Gamma\sigma + \gamma_1\beta]H(r-r_i), \\ 0 &= \dfrac{D_2}{r^2}\dfrac{\partial}{\partial r}\left(r^2 \dfrac{\partial \beta}{\partial r}\right) - \gamma_2\beta H(r-r_i), \end{cases} \tag{5}$$

with N the rate at which necrotic cells disintegrate and γ_1 and γ_2 the rates at which the inhibitor decays within the proliferative and necrotic regions, respectively. All other notation equates with that in models (1) and (4) with one exception—in model (5), Γ represents the consumption rate of nutrient by living cells. Furthermore, nutrient is delivered to the interior by diffusion from the media or interstitium, not through an interior vascular network as in (4). There is no quiescent layer in either model.

Among the advances introduced by models (4) and (5) is a more realistic action for the inhibitor. Instead of causing quiescence, the inhibitor is hypothesized to increase cell mortality within nonnecrotic regions of the spheroid, which Byrne and Chaplain equate to apoptosis. Therefore, $S(\sigma,\beta)$ is interpreted as pointwise differences between births and deaths and generally increases with σ and decreases with β. This hypothesis allows richer dynamics than Greenspan's model. Of particular importance, model (4) shows that spheroids can reach a steady state without necrosis. (See [29, 38] for more details.) In fact, a sufficiently large apoptosis rate can cause complete spheroid regression without development of a necrotic core in both models. Model (5) also predicts that spheroids with a necrotic core arise only if loss to apoptosis is less significant than loss to necrosis and if the external oxygen concentration is not too large. More precisely, they show that for a particular realization of g_1 and g_2, the width of the proliferating rim is proportional to $\sqrt{\sigma_\infty - \sigma_l}$, where σ_∞ is the nutrient concentration in the media and σ_l is defined above.

More recently, Davide Ambrosi and Francesco Mollica [6, 7] modeled nutrient deficiency in multicell spheroids cultured either free in suspension or embedded in agarose. These models introduce mechanical stress generated within the tumor and

externally through the agarose gel under the assumption of an elastic spheroid. As in the previous models, nutrient is assumed to diffuse into the spheroid from the media very rapidly relative to cell proliferation rates. Since Ambrosi and Mollica imagine the nutrient to be a storable form of energy to power cell proliferation, one can interpret it as glucose. They assume that glucose determines reproductive potential of cells within the spheroid. In particular, if we let n be the nutrient concentration and g be the growth potential (birth rate minus death rate) at a certain point within the spheroid, then g is an increasing linear function of glucose concentration such that $g(n,\cdot) < 0$ for $0 \leq n < n_0 < \infty$, reflecting the dominance of deaths over births in low-glucose environments. In addition, g decreases with a measure of stress on the cells.

The complexity of Ambrosi and Mollica's formalism takes a complete description of their model outside the scope of this review. However, their results are of interest. Numerical investigations show that the spheroid naturally develops an outer proliferative rim with a core dominated by lack of nutrient. Predictions about necrosis per se cannot be made from their analysis, because they chose $n_0 = 0$. However, their formalism hints at the possibility of combining the nutrient-deficiency and mechanical-deformation hypotheses (see section 3.3) into a single model, which promises an incisive instrument to tease these two hypotheses apart.

3.2.2. *Diffusion limitation in tumor cords.* The tumor cord is a concept introduced around the same time that theorists started modeling multicell spheroids [54, 110]. In essence, the tumor cord turns the spheroid inside-out, placing the source of nutrient in the center, and transforms it from a sphere to a cylinder. The cord itself is a sleeve of tumor tissue surrounding a microvessel, which supplies nutrients and waste removal services. The outer portion of the cord is often necrotic (Fig. 3). Tumor cords can be observed in certain regions of certain tumors (see [57] for example) but not all (see Fig. 1 for example).

Recently, Alessandro Bertuzzi, Alberto Gandolfi, and their colleagues [13, 15, 16] (reviewed in [14]; see also [33]) have studied tumor cords theoretically. In their models, we imagine a rigid-walled capillary of radius r_0 surrounded by a cylinder of tissue. The maximum (fixed) width of the cord is R. In later work, they also introduce a necrotic rind of outer radius B. As in the spheroid models above, surface tension and incompressibility of cells and interstitium maintain the cord's shape, and the tissue can exist as a mosaic of both proliferative and quiescent cells. The rate at which cells become quiescent decreases with local nutrient concentration. However, a distinct annulus of quiescent cells can arise when nutrient concentration falls below a prescribed threshold. In some of these models, the active cell population is structured by age. Within the tissues, both living and necrotic, the volume is entirely exhausted by three components: living cells (ν_p), necrotic cells (ν_n), and extracellular space (ν_e). Cell packing is assumed to be homogeneous (ν_e and $\nu_p + \nu_n + \nu_e$ are constants).

These assumptions lead Bertuzzi et al. [13] to a model that really consists of two submodels for the cell dynamics. The first, expressed generally as

$$\begin{cases} \dfrac{\partial \nu_p}{\partial t} + \nabla \cdot (\mathbf{u}\nu_p) &= \chi(\sigma)\nu_p - [\mu(\sigma) + \mu_c(c,\sigma) + \mu_r(\sigma,t)]\nu_p, \\ \dfrac{\partial \nu_n}{\partial t} + \nabla \cdot (\mathbf{u}\nu_n) &= [\mu(\sigma) + \mu_c(c,\sigma) + \mu_r(\sigma,t)]\nu_p - \mu_n\nu_n, \end{cases} \tag{6}$$

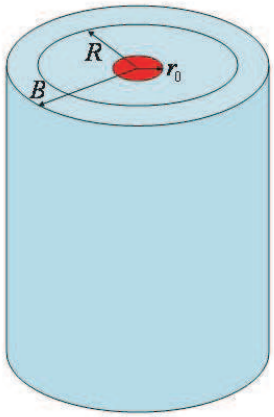

FIGURE 3. Idealized section of a tumor cord. The red core represents a microvessel with radius r_0. Surrounding the vessel is a sleeve of living tumor tissue with outer radius R that is further surrounded by a necrotic rind of radius B. Based on Fig. 1 of [14, p.163].

describes dynamics in the region of living tissue ($r_0 < r < R$). The second,

$$\frac{\partial \nu_n}{\partial t} + \nabla \cdot (\mathbf{u}\nu_n) = -\tilde{\mu}_n \nu_n, \tag{7}$$

valid for $R < r < B$, models the necrotic region, because no living cells are present there ($\nu_p \equiv 0$). The vector $\mathbf{u}$ represents a cell velocity field that arises as cells push on one another as they reproduce or are squeezed together as some disintegrate. If one assumes that this motion is confined to the radial plane in a perfect cylinder, then $\mathbf{u} = u(r)$, where r is the radial position. In addition, $\chi(\sigma)$ is the per-capita proliferation rate, which depends on nutrient concentration σ; $\mu(\sigma)$ is the "natural" mortality rate; and μ_n and $\tilde{\mu}_n$ represent the disintegration rate of necrotic cells in living tissue and the necrotic rind, respectively. The additional death terms $\mu_c(c,t)$ and $\mu_r(\sigma,t)$ denote death rates from chemotherapeutics and radiation treatment, respectively, where c is the drug concentration. The dependence of μ_r on σ arises because the authors assume the nutrient is oxygen, and radiation-induced mortality is well known to depend on local O_2 concentration [54].

Nutrient is assumed to move entirely by diffusion on a much faster time scale than cell velocity. Therefore, they assume that

$$\Delta\sigma = f(\sigma)\nu, \tag{8}$$

where f depends on the diffusivity of O_2 and the rate at which the tissue consumes it. Nutrient enters the cord only across the microvessel wall at a constant rate, reflecting blood O_2 homeostasis. They also impose a no-flux condition for O_2 at the outer cord boundary. As with the spheroid models, these authors assume that all cells become necrotic whenever O_2 concentration falls below some threshold σ_n.

Cells enter a reversible quiescent state, modeled in $\chi(\sigma)$, if O_2 drops below another threshold, $\sigma_q > \sigma_n$.

Interestingly, this model predicts that the boundary between necrotic and living tissue cannot always be identified as the point at which σ drops below σ_n. For example, suppose the cord sits at its steady-state radius with the demarcation of its necrotic region r_n defined by $\sigma(r_n) = \sigma_n$. Suppose further that a chemotherapeutic attack kills a large number of tumor cells. Afterward, competition for oxygen among survivors transiently slackens, and the cord begins to grow, pushing the necrotic region outward. Then for a short period the boundary of the necrotic region is determined by history and not by nutrient availability. One can therefore in principle use this model to predict the transient dynamics of a tumor cord following cytotoxic treatment as a way to test the hypothesis that necrosis is caused by a lack of O_2 or, with proper modification, some other nutrient. More mundane phenomena, in particular the size of the viable and necrotic sleeves as a function of O_2 delivery, can be used for a similar purpose, at least in principle.

3.2.3. *Diffusion limitation in ductal carcinoma in situ.* Whole autochthonous tumors are often much more difficult to model than laboratory systems, such as multicell spheroids, or special in vivo systems, such as tumor cords or explants, because their geometries are usually much more irregular. However, breast ductal carcinoma in situ (DCIS) is something of an exception and so has attracted the attention of mathematical oncologists [37, 117]. By definition, this lesion is confined to the lumenal side of the duct's basement membrane, which means it is usually forced to grow in a cylindrical shape around 700 μm in diameter on average [37]. Unlike tumor cords, however, nutrients are delivered to the cancer cells via diffusion from the external surface of the cylinder rather than a central blood vessel.

A recent model of early DCIS by Susan Franks et al. [37], although including no explicit mechanism of necrosis, helps explain why some such lesions have a necrotic interior that others lack. In their investigation, they imagine a tumor growing within a rigid-walled cylinder representing a milk duct. Tumor cell proliferation therefore generates pressures that force cells to move with velocity $\mathbf{v}(\mathbf{x})$ at point $\mathbf{x}$. The portion of the model describing tumor volume and nutrient concentration takes the following form:

$$\begin{cases} \dfrac{\partial n}{\partial t} + \nabla^2 \cdot (n\mathbf{v}) &= D_n \nabla^2 n + (k_m(c) - k_d(c))n, \\ \dfrac{\partial m}{\partial t} + \nabla^2 \cdot (m\mathbf{v}) &= D_m \nabla^2 m + k_d(c)n, \\ \dfrac{\partial \rho}{\partial t} + \nabla^2 \cdot (\rho\mathbf{v}) &= D_\rho \nabla^2 \rho, \\ \dfrac{\partial c}{\partial t} + \nabla^2 \cdot (c\mathbf{v}) &= D_c \nabla^2 c + -\beta k_m(c)n, \end{cases} \tag{9}$$

where n and m are densities of living and dead cells, respectively; ρ is the density of interstitial fluid; and c is nutrient concentration. Functions k_m and k_d represent per-capita births and deaths, respectively. Generally, k_m increases with c, and k_d decreases with c. Diffusion coefficients are represented as D_i, $i \in \{n, m, \rho, c\}$, and β is the amount of nutrient required to produce a new cell. Dead cells never disintegrate, and living, nondividing cells do not consume nutrient. By assuming that the tumor mass is exhausted by living cells, dead cells, and interstitial material,

they show that

$$\nabla \cdot \mathbf{v} = k_m(c)n. \tag{10}$$

They then complete the model by using Stokes's law to derive expressions for intratumoral pressure.

This model produced no necrosis, because the duct diameter was so small that nutrient concentration favored proliferation over mortality everywhere in the tumor interior. However, the authors point out that allowing the duct wall to distend will decrease nutrient concentration in the tumor core, perhaps to the point where necrosis develops, as in comedocarcinoma [64], for example. The model could be extended to allow one to probe this scenario empirically, either in animal models or human histopathology samples, as a test of the nutrient-deficiency hypothesis.

3.3. **Necrosis caused by mechanical disruption of cells.** In distinct contrast to the nutrient-limitation hypothesis, Colin Please et al. [93, 94] hypothesize that necrotic regions form because cells are torn from their anchors to the extracellular matrix (ECM) and each other by pressures within the tumor. This mortality could arise either from literal destruction of the plasma membrane or apoptosis caused by loss of cell-ECM or cell-cell contact. The basic models [93] assume that the tumor's interior consists of two "phases"—cells and interstitial fluid. (ECM is not explicitly modeled in these early explorations.) Please et al. assume that cell interiors are composed of the same material as the interstitial fluid; therefore, fluid moves between phases, entering cells through the process of proliferation and reentering the interstitium as dead cells disintegrate. The models are thereby controlled primarily by conservation of this fluid. The requirement for fluid conservation produces pressures within the tumor that cause both cell and fluid movement. For example, as cells proliferate, fluid entering the cell phase produces an "outward" pressure, pushing the cell phase outward. Cells move freely in response to this force, because unlike the previous models, cells in this system do not adhere to each other. On the other hand, pressures in the fluid phase force interstitial fluid to move among the cells as if the tumor were a porous medium. Therefore, two pressures must enter the model: (1) the pressure on the interstitial fluid (P_e) and (2) the pressure exerted cell-to-cell via the ECM scaffold (P_c). The intracellular pressure is not modeled.

If in any region within the tumor $P_c > P_e$, then the cells in that region feel a compressive force through the surrounding ECM. If the inequality is reversed, then cells are assumed to be torn apart as tension forces rip them from the ECM. Although Please et al. hypothesize that this form of cell destruction occurs only to physiologically stressed cells, as in hypoxia, in the model any cell in such an environment is destroyed. This, then, is the mechanism of necrosis under investigation.

Although nutrient deficiency does not cause necrosis here, nutrients still play a role. As before, the nutrient moves primarily by diffusion on a much faster time scale than cell kinetics, so the nutrient concentration, denoted $C(\mathbf{x})$, is assumed to be in a quasi-steady state. Please et al. assume that cells proliferate at a rate proportional to the nutrient concentration and die at a constant per-capita rate; that is, at $\mathbf{x}$ the per-capita growth rate density is $dC(\mathbf{x}) - e$. If we let k be the constant permeability of fluid through the interstitium and ϕ be the proportion of the tumor volume taken up by interstitial space, also assumed to be constant throughout the tumor, then the above assumptions can be modeled as follows [94]:

$$k(1-\phi)^2\nabla^2 P_c = e - dC. \tag{11}$$

Consider the application of this model to a multicell spheroid. Again we assume perfect spherical symmetry and a nutrient diffusing into the spheroid from the external media (see [94] for the detailed boundary conditions). Then once again dynamics vary only over the radial position, so we can replace $\mathbf{x}$ with r defined in section 3.1. In this case, the O_2 concentration obeys the following relation:

$$C(r,t) = \frac{R_0[\sinh(r-R_i) + R_i\cosh(r-R_i)]}{r[\sinh(R_0-R_i) + R_i\cosh(R_0-R_i)]}, \tag{12}$$

with R_0 and R_i defined as in section 3.1 except that the necrosis condition is now $P_c < P_e$. In addition, the tumor and necrotic radii must satisfy the following conditions:

$$R_0^2\frac{\mathrm{d}R_0}{\mathrm{d}t} = \int_{R_i}^{R_0} r^2(C(r,t)-\alpha)\,\mathrm{d}r, \tag{13}$$

$$0 = \int_{R_i}^{R_0}\left(r - \frac{r^2}{R_0}\right)(C(r,t)-\alpha)\,\mathrm{d}r, \tag{14}$$

where $\alpha = e/dC(R_0)$.

Superficially this model predicts observed spheroid behavior. Starting with a small spheroid, the radius grows exponentially until the moment a necrotic core begins to develop in the center. At that time, it enters a "linear" growth phase with a necrotic core eventually growing at the same rate, producing the proper histology. The depth of the proliferative layer will in general differ from that predicted by nutrient-deficiency models and can therefore be used to contrast the two hypotheses empirically.

Unfortunately, this model makes a disturbing prediction—in the absence of surface tension, the spheroid grows without bound. In fact, this result is general across choices of cell-growth models as long as cell proliferation is nondecreasing with oxygen concentration. However, Please et al. show in [94] that one can relax the assumption of inviscid cells and allow a (small) surface tension that can halt runaway growth. Doing so requires only the addition of the term $2\Gamma/R_0$ to equation (14), where Γ is a measure of surface tension.

Working from an extension [62] of the previous model, C. Y. Chen et al. [27] investigate the mechanical disruption hypothesis in spheroids growing in agarose gels. The gel is assumed to be elastic and therefore exerts pressure on the spheroid as it grows. Once again the tumor consists of cellular and extracellular fluid phases permeated by a nutrient, all of which obey the following relations:

$$\begin{cases} \dfrac{\partial\psi}{\partial t} + \nabla\cdot(\psi\mathbf{U}_c) = \psi S(C), \\ \dfrac{\partial(1-\psi)}{\partial t} + \nabla\cdot[(1-\psi)\mathbf{U}_e] = -\psi S(C), \\ D\nabla^2 C = \psi\Sigma(C), \end{cases} \tag{15}$$

where ψ is the cellular volume fraction within the tumor ($\equiv 1-\phi$ for ϕ defined above); $\mathbf{U}_c$ and $\mathbf{U}_e$ represent velocity fields for cell and extracellular fluid, respectively; S denotes cell-growth rate; D is oxygen diffusivity through the tumor; Σ represents rate of nutrient consumption; and all other notation is defined earlier in this section. Following [62], Chen et al. include in the force balance equations hydrodynamic drag, hydrostatic forces in the interstitial fluid, and forces among cells transmitted by an ECM scaffold. In the nonnecrotic region, by definition $P_c > P_e$

and cells are maximally packed such that $\psi = \psi_0$, ψ_0 a constant; however, in the necrotic core, $P_e = P_c$ but $\psi \leq \psi_0$.

The model becomes quite tractable if one limits the investigation to a perfect sphere, defines $\Sigma(C) = 1$, and sets

$$S(C) = \begin{cases} 1 & \text{if} \quad C > \alpha, \\ -\rho & \text{if} \quad C \leq \alpha, \end{cases} \tag{16}$$

where α represents a lower O_2 threshold below which cell death predominates and ρ is a positive constant representing sensitivity of cells to nutrient deficiency. With this definition of the growth function, spheroids obeying model (15) can develop three histologically distinct regions: a necrotic core, a middle annulus characterized by cell mortality dominating proliferation, and an outer annulus of proliferative tissue. As in [94], this model predicts that spheroids suspended in liquid media (zero gel stiffness) obtain the traditional histology, including a necrotic core, but contrary to observation tend to grow without bound. In a gel, however, spheroids always asymptotically approach a limited size, with or without a necrotic core.

For our purposes the most important prediction made by this model involves the relationship of necrosis to gel stiffness. In a very rough sense, spheroids in stiffer gels tend to be smaller at their steady-state size, with a lower likelihood of becoming necrotic than spheroids in more elastic gels. Even if necrosis does develop, it tends to arise later in stiffer gels. Apparently, stiff gels squeeze fluid out of the spheroid while favoring cell compression, so the necrosis conditions are less likely to be met. Therefore, this model encourages one to test the mechanical disruption hypothesis against nutrient deficiency by varying gel stiffness and nutrient availability using a fully crossed, factorial experimental design. (See [55] for example.)

3.4. **Necrosis from local acidosis.** A series of recent investigations by Robert Gatenby and his colleagues focusing on how malignant neoplasms invade surrounding tissue has also produced an explanation of necrosis that harkens back to the inhibitors hypothesized by Greenspan, Byrne, and Chaplain. In this case, Gatenby and his colleagues identify the inhibitor as acid. Most malignant tumors acidify their local environments because parenchyma cells metabolize glucose via glycolysis and fermentation, which produces lactic acid that cells then secrete [43, 45, 97] (see section 4.2.2 for an elaboration of this idea). Gatenby et al. [41, 42, 90] suggest that this acidification selects for tumor cells able to withstand acidosis, allowing them to outcompete and therefore invade adjacent healthy tissue. In one model of this hypothesis [41, 42], one represents the densities of cancer and healthy cells with $N_1(\mathbf{x}, t)$ and $N_2(\mathbf{x}, t)$, respectively, at point $\mathbf{x}$ in the tumoral or peritumoral environment at time t. The excess hydrogen ion or lactic acid concentration is denoted $L(\mathbf{x}, t)$. With this notation, Gatenby et al.'s model becomes

$$\begin{cases} \dfrac{\partial N_1}{\partial t} &= r_1 N_1 \left(1 - \dfrac{N_1}{K_1} - \alpha_{12} \dfrac{N_2}{K_2}\right) - d_1 L N_1, \\ \dfrac{\partial N_2}{\partial t} &= r_2 N_2 \left(1 - \dfrac{N_2}{K_2} - \alpha_{21} \dfrac{N_1}{K_1}\right) - d_2 L N_2 + \nabla \cdot [D_{N_2} \nabla N_2], \\ \dfrac{\partial L}{\partial t} &= r_3 N_2 - d_3 L + D_L \nabla^2 L, \end{cases} \tag{17}$$

where d_1 and d_2 are excess death rates of the two cell types due to local acidosis; $D_{N_2}(N_1, N_2)$ represents cancer cell motility, modeled in particular as either $D_2(1 - N_1/K_1)$ or $D_2(1 - N_1/K_1 - N_2/K_2)$; r_3 is the per-cancer-cell H^+ secretion

rate; d_3 is the rate at which hydrogen ions wash out in blood or are absorbed by physiological buffers; and D_L is the acid diffusivity through tumor tissue. A cellular automaton (CA) analogue of this system, with an addition of glucose delivery through a vascular net, has also been studied [42, 90].

Both model (17) and its CA analogue support the notion that acid secretion facilitates invasion, even in small tumors. These models also suggest a relationship between the morphology along the tumor edge and invasiveness; namely, a gap between tumor and healthy tissue tends to form in more aggressively invasive cancers. More important for our current purposes is the observation of necrosis in the CA model. Under certain circumstances, Aalpen Patel et al. [90] show that areas within the tumor can become so acidic that all cells are destroyed, yielding a region of necrosis.

Although this mechanism is distinctly different from all others presented above, it may be hard to tease apart from the nutrient limitation hypothesis for the following reason. Cancer cells might evolve to rely on glycolysis instead of the tricarboxylic acid cycle precisely because of nutrient limitation in nascent tumors [43, 45]. So areas where nutrients are limited are precisely those areas where selection favors cells that acidify the environment, resulting in a spatial correlation between nutrient deficiency and acidosis. However, the acidification hypothesis predicts that in older tumors at least regions with a higher density of parenchyma cells and therefore regions of high acid secretion, should be more prone to necrosis than regions with a more mixed histology, even if nutrient delivery does not vary between the areas. Models such as (17) and those presented in sections 3.2 and 3.5 may be employed to refine this prediction into something empirically testable.

3.5. **Necrosis due to local ischemia.** The irregular pattern of necrosis often observed in real tumors begs for more complex hypotheses than those presented above. In particular, how necrosis-inducing conditions arise in larger, irregularly shaped tumors in the face of vascularization needs explanation. If necrosis is caused by nutrient limitation, for example, then what determines where it occurs within a vascularized tumor? If, on the other hand, mechanical disruption of cells causes necrosis, then can one predict where such necrotic regions will crop up within a growing tumor given its location within the body?

To my knowledge, no major theoretical work has been done on the mechanical-disruption hypothesis in an in vivo setting, probably for two reasons. The first is the obvious complexity involved; the region of the body itself would have to be modeled, including organ shape and tissue compositions. The importance of these factors is highlighted by the observation that multicell spheroid behavior depends in part on the stiffness of the media (see section 3.3). Second, the hypothesis itself is relatively young and so has not been fully analyzed beyond the simplified geometry of a spheroid.

On the other hand, three distinct variations of the nutrient-limitation hypothesis have been proposed to explain necrosis in vascularized tumors. All three point to local ischemia (lack of blood delivery at the tissue level) as the culprit, but they disagree on what causes the ischemia. One, commonly cited in oncology texts, suggests that tumors "outgrow their blood supply"; that is, parenchyma growth exceeds vascular growth in some region within the tumor, resulting in a local ischemic necrosis. The viability of this hypothesis is questionable, because the net proliferation rate appears to depend on local perfusion, so it is unclear how the parenchyma could overshoot its local "carrying capacity" so wildly. Nevertheless,

such a mechanism could account for some subtle oscillations in growth rate [82] (see section 5 below). In the second variation, local ischemia is caused by compressive pressure within the tumor, which collapses tumoral blood vessels. This compression is thought to arise in part through high fluid pressure in the interstitium [76], although bulk pressure from cells probably plays a dominant role [59]. Finally, the third variation places the blame on irregular distributions of blood flow and hematocrit that can arise even within a highly organized microvascular net. Here, I will focus on models of these last two variations.

3.5.1. *Ischemia caused by vascular collapse.* One version of this hypothesis has been modeled by Mollica et al. [76] at the level of a single microvessel. In this model we imagine a capillary of length L situated within the tumor. The interstitial fluid pressure, π_i, is assumed to be constant, so the pressure acting on the capillary at location x along its length at time t, denoted $p(x,t)$, is $\pi(x,t) - \pi_i$, where π represents the vessel pressure. If $p < 0$, then the capillary feels a compressive force and will begin to collapse. Sufficient compression causes the capillary to buckle, resulting in almost complete cessation of blood flow. On the other hand, the capillary is assumed to have some elasticity, so it may dilate in response to the distending force the capillary feels when $p > 0$.

If we let $u(x,t)$ be the displacement of the capillary wall from its average width h_0, then the main model equations take the following form:

$$\begin{cases} -\dfrac{T}{w}\dfrac{\partial^2 u}{\partial x^2} + \Phi(u) - p + c\dfrac{\partial u}{\partial t} + \rho H \dfrac{\partial^2 u}{\partial t} = 0, \\ -\dfrac{\partial}{\partial x}\left((h_0+u)^3 \dfrac{\partial p}{\partial x}\right) + \dfrac{3kp}{w\delta} + \dfrac{3\mu}{w}\dfrac{\partial u}{\partial t} = 0, \end{cases} \tag{18}$$

where T represents capillary wall tension, w normalizes the vessel cross section so changes in its area can be equated to changes in the height of a rectangle of equal area, $\Phi(u)$ represents the capillary wall stiffness, c is a drag coefficient, ρ represents interstitial fluid density, H is the virtual mass coefficient, δ is the capillary wall's thickness, k denotes the permeability of the capillary wall to serum, and μ is blood viscosity. At the venous and arterial ends, the capillary is held at fixed width h_0, and the entrance (arterial, π_a) and exit (venous, π_v) pressures are also fixed, with $\pi_a > \pi_v$.

Numerical investigation of this model uncovered a regime in which blood flow through the vessel cycles on a 100-millisecond time scale. The cycles appear to be chaotic and persistent, indicating a continuous "pulsing" of blood through the capillary independent of the cardiac cycle, which was not modeled. The original purpose of the model was to investigate observed variation in blood flow rate and direction in actual tumors. Mollica et al. note that their results, while intriguing, fail to explain observed behavior because the oscillations occur much too rapidly. However, they suggest that a network of such capillaries and relaxation of certain simplifying assumptions may yield more realistic behavior. A similar cautionary remark applies to the use of this model to study necrosis. The basic premise is promising, but a more coarse-grained scale is probably required. Nevertheless, this model is an important mechanistic attack on the problem.

3.5.2. *Ischemia caused by irregular blood flow and hematocrit distributions.* Although it is well-known that tumors frequently suffer disrupted circulation [59, 97], vessel collapse from compressive pressure is not the only possible mechanism.

Tomas Alarcón et al. [3, 4] investigate an alternative in which ischemia arises as a result of capillary accommodation responses and heterogeneous distribution of hematocrit throughout a tumor. Using a "hybrid" cellular automaton model, so called because it includes a traditional diffusion formalism along with the CA mechanism, they study the effects of heterogeneous blood distribution on the competition between tumor cells and healthy cells. The setting is a prescribed, two-dimensional vascular net overlaying a 60-by-60 pixel CA grid. Each pixel in the grid represents one (biological) cell, so the domain is about 1200 μm^2, assuming an average cell diameter of 20 μm. The vascular bed is a regular "hexagonal" net with anastamoses every 80 to 90 μm or so. This arrangement results in a maximum avascular interval of 160 μm along the vertical axis and 240 μm along the horizontal.

The vessels themselves are not inert tubes. Rather, they change diameter in response to changes in transmural pressure, sheer stress, effective oxygen delivery and intrinsic mechanisms. In short, if we let $R_{i,t}$ be the diameter of the ith capillary section at time step t, then accommodation dynamics of the capillary are described by the following equation, which because of the CA formalism is expressed in discrete time steps of length Δt:

$$\frac{R_{t+\Delta t} - R_t}{\Delta t} = R\left[\ln\left(\frac{\tau_w}{\tau(P)}\right) + k_m \ln\left(\frac{\dot{Q}_r}{H\dot{Q}} + 1\right) - k_s\right], \tag{19}$$

where the i subscripts have been dropped, τ_w is the sheer stress along the capillary wall, $\dot{Q}$ is whole blood flux, $\dot{Q}_r$ measures constant oxygen demand of cells serviced by the capillary, k_m measures how sensitive the capillary response is to discrepancies between O_2 demand and O_2 delivery, and k_s represents an innate tendency of the capillary to shrink in the absence of other modifiers. In addition, the authors assume that capillaries homeostatically regulate sheer stress around a set point that can vary with transmural pressure, P; that set point is represented by $\tau(P)$ and was determined empirically. The variable H is a measure of red blood cell count or, alternatively, moles of O_2 and can be thought of as proportional to the hematocrit, the red cell volume fraction of whole blood.

The most important aspect of this paper is the recognition that hematocrit tends not to remain homogeneous in a microvascular net; therefore, if hematocrit in one region of a tumor became very low, nutrient delivery would be impaired and necrosis might result. The mechanism causing hematocrit inhomogeneity is the tendency of erythrocytes to disproportionately enter branches with larger flow rates per unit area in the branch's cross section. To model this phenomenon, Alarcón et al. assume that at a vessel bifurcation, erythrocytes prefer to enter branches with a larger flow rate. In fact, if the difference in flow rates is large enough, all erythrocytes enter the faster branch.

Results of this model showed that both blood volume and hematocrit can vary wildly throughout a microvascular net. Unfortunately, Alarcón et al. did not use this model to investigate it as a mechanism of necrosis, but certainly this intriguing hypothesis is worth following up.

4. **What causes cell diversity within malignant neoplasia?** Along with necrosis, cell diversity is another biologically and clinically significant feature of malignant neoplasia, the explanation of which benefits from an ecological perspective. This cellular diversity exists on two levels. The first, which for convenience I will

call "Type I" diversity, includes all types of cells within malignant tumors, including parenchyma cells, "healthy" cells of the reactive stroma—primarily fibroblasts and myofibroblasts—and cells of the circulatory infrastructure—blood and lymph endothelial cells, pericytes, smooth muscle cells, and a few others. In addition, immune reactive cells, including lymphocytes, macrophages, and neutrophils, are also present (Fig. 1).

The second type of diversity, "Type II," is variation in parenchyma cell anatomy and physiology. Anatomical variation alone is typically referred to as cellular pleomorphism, or more specifically nuclear pleomorphism if one focuses on that organelle, but here I will extend the concept to include physiological differences as well. Although mathematical attacks on the causes of necrosis have a deeper history than studies of tumor cell diversity, theories for both types have appeared, as I review below.

4.1. **Causes of Type I diversity.** Cancer can be understood as a result of natural selection favoring certain cell lineages that one can describe as "selfish 'cheats' that exhibit antisocial characteristics" [84, p.493]. In the short term, selection favors aggressive mutant cells over "healthy," cooperating cells at the expense of integrated tissue architecture. Tissue integration breaks down because mutant cells enter a competition for resources that otherwise would not exist among cooperating, genetically similar clones. Since this destruction of tissue architecture, which defines malignancy, arises through disrupted relationships among all cell types within the lesion, Type I diversity should be a major focus, if not the main focus, of theoretical oncology. However, besides efforts to model angiogenesis (see [8, 25, 26, 65, 66, 72, 92, 102] for reviews) and some promising recent models of interactions between parenchyma and ECM [26], the most modern empirical research of phenomena at this level of diversity (which can be thoroughly explored in [17, 32, 58, 67, 71, 89, 96, 98, 100, 114]) has attracted surprisingly little attention from the theoretical oncology community.

Despite the relative paucity of effort directed at Type I diversity, at least three hypotheses explaining how it arises can be derived from existing research. The first suggests that invading parenchyma cells cannot entirely outcompete the original healthy population, leaving remnants of the healthy population in pockets or spread evenly throughout the tumor. The second supposes that tumor tissue invades surrounding healthy tissue with fingerlike projections, like the fungiform invasion described in pathology texts, caused by known reaction-diffusion mechanisms. Finally, the third hypothesis is an extension of the first. Complex interactions among parenchyma, healthy, and immune cells within the lesion cause Turing-like patterns to arise in which densities of the various cell types vary throughout the tumor, with some areas inhabited primarily by parenchyma, others by normal cells. Each of these ideas is explored more fully below.

4.1.1. *Incomplete competitive exclusion.* Perhaps the most straightforward way to represent the competition among cell types characteristic of malignancy is a direct application of the Lotka-Volterra model, as was made by Gatenby [40]:

$$\begin{cases} \dfrac{\mathrm{d}N}{\mathrm{d}t} &= r_N N\left(1-\dfrac{N+\alpha T}{K_N}\right), \\ \dfrac{\mathrm{d}T}{\mathrm{d}t} &= r_T T\left(1-\dfrac{T+\beta T}{K_T}\right), \end{cases} \tag{20}$$

where $N(t)$ and $T(t)$ represent the number of healthy cells and tumor cells, respectively; K_i is the "carrying capacity" for a body made exclusively of cell type i; α measures the competitive impact of tumor cells on healthy cells; β is the competitive impact of healthy cells on tumor cells; and r_i is the intrinsic rate of increase for cell type i. The dynamics of this model are well understood [56, 80]; the novelty is Gatenby's interpretation of the behaviors. He views parameter regions that allow an attracting interior (nonboundary) fixed point as benign neoplasia. Malignancy is recognized as an attracting fixed point on the boundary for which $N = 0$ and $T = K_T$. Later, Gatenby et al. [44] used this system in a general reaction-diffusion model,

$$\frac{\partial \mathbf{n}}{\partial t} = \mathbf{f}(\mathbf{n}) + D\nabla^2\mathbf{n}, \tag{21}$$

where $\mathbf{n}(\mathbf{x}, t)$ is a vector of cell population densities for all cell types at point $\mathbf{x}$ and time t, D is a matrix of cell motility coefficients, and $\mathbf{f}(\mathbf{n})$ is a generalization of model (20) that includes an arbitrary number of cell types competing at a point in space. In their application, Gatenby et al. limit the model to one space dimension and two competing species, again cancer versus healthy cells, so $\mathbf{f}(\mathbf{n})$ is the right-hand side of model (20).

Again, model (21) is well studied [81] and known to admit travelling-wave solutions with well-characterized velocities, interpreted by Gatenby et al. as tumor invasion of surrounding tissue. In particular, if

$$\alpha K_T > K_N \tag{22}$$

and

$$\beta K_N < K_T, \tag{23}$$

then the tumor will invade surrounding healthy tissue, completely replacing it, at a speed no less than

$$2\sqrt{r_T D_T \left(1 - \frac{\beta K_N}{K_T}\right)}. \tag{24}$$

However, if the inequality in equation (23) is reversed, then the tumor still invades but does not entirely eliminate surrounding healthy tissue. This result is interpreted as desmoplasia, a mixture of cancerous and noncancerous cells within a tumor. Therefore, this model explains tumor cell diversity as incomplete competitive exclusion.

This model, although simple, makes some interesting practical predictions about how tumors will respond to treatment. Most basically, any successful treatment must reverse both inequalities (22) and (23). If the treatment is successful and scar-forming tissue has essentially the same properties as the original healthy tissue destroyed by the tumor, then the lesion will scar over at a minimum speed given by an expression formally equivalent to (24), with subscripts switched and α replacing β. Also, as Gatenby et al. point out, cytotoxic therapy can kill tumor cells directly and may blunt the tumor population's intrinsic rate of increase r_T. In neither case will it have an effect on the asymptotic behavior of the tumor—r_T does not determine the stability properties of the steady states—unless the tumor is entirely eradicated. Such behavior in the model may help explain why cytotoxic therapy often fails.

Gatenby et al. use this insight to identify other parameters that might make more promising targets for therapy. In fact, this model supports attacks on a potential target already identified—tumor vasculature [36]. In the context of this model, an

attack on tumor angiogenesis at the least reduces K_T, which will tend to reverse both inequalities (22) and (23). If all else remains equal, angiogenesis inhibition could therefore cause stability of the boundary equilibria to switch, in which case the tumor would regress *without further cytotoxic treatment*. In essence, the body itself would destroy the tumor by outcompeting it. However, whatever effect such a treatment has on K_T, it must not equally degrade K_N, as is clear from relations (22) and (23).

These inequalities also suggest that one might profitably attack the tumor by altering the competitive relationship between cancerous and healthy cells since decreasing α and increasing β will also tend to favor healthy cells. Gatenby et al. suggest that techniques to decrease tumor cell nutrient uptake and perhaps increase healthy cell uptake might work. This idea is in line with results obtained by [60]. Gatenby et al. also recommend looking for ways to decrease protease expression and acid secretion as ways to decrease α. They also suggest one might consider trying to increase K_N by somehow attenuating contact inhibition among normal cells.

4.1.2. *Fungiform invasion.* As an alternative to the incomplete-competitive exclusion hypothesis, a model by Shusaku Tohya et al. [107] suggests that nutrient dynamics within the tumor drives Type I diversity. This model was originally designed to explore the irregular penetration of dermis by nodular lesions of basal cell carcinoma (BCC), a largely curable form of skin cancer. In this model, we look at a cross section through a BCC lesion perpendicular to the skin. All dynamics occur on the plane of the cut, so it is convenient to let x and y be the dimensions parallel and perpendicular to the skin's surface, respectively. Also, let $0 \leq x \leq X$ and $0 \leq y \leq Y$. Nutrient is delivered to the tumor by a capillary that lies along the basal edge of the tumor, so the nutrient along the line $y = Y$ for all allowable x is fixed at n_0. Cells take up this nutrient, metabolize it, and use it for both movement and growth. If we let $n(x, y, t)$ and $c(x, y, t)$ be the nutrient concentration and cancer cell density, respectively, at point (x, y) and time t, then Tohya et al.'s model becomes

$$\begin{cases} \dfrac{\partial n}{\partial t} &= D_n \nabla^2 n - knc, \\ \dfrac{\partial c}{\partial t} &= \nabla(D_c(n,c)\nabla c) + \theta f(n,c), \end{cases} \tag{25}$$

where D_n is the diffusivity of nutrient; k is the base rate at which cells uptake and metabolize nutrient; $D_c(n, c) = \sigma nc$, σ constant, expresses cancer cell motility; and θ measures how efficiently cells convert nutrient into new growth. Initially the lesion starts as a flat layer of cells of fixed thickness y_0, with the remaining space $y_0 < y < Y$ for all allowable x considered to be normal dermal tissue.

Despite this model's formal simplicity, it produces an intriguing hypothesis. Under certain conditions, in particular when $n_0\sqrt{\theta/D_n}$ is sufficiently small, the lesion extends tumorous "fingers" into the dermis. If sectioned in any way other than exactly perpendicular to the skin surface, a microscopic examination of such tissue would look like islands of normal tissue within a sea of cancer tissue, or vice versa. Alternatively, it is not hard to imagine a more realistic extension of model (25) in which these fingers grow together, engulfing islands of healthy tissue and yielding a realistic histology. As it stands, the simulations make certain predictions about the width of the tumorous fingers and the rate at which they grow as functions of parameters that may help guide empirical investigation.

4.1.3. *Turing instabilities.* A model by Markus Owen and Jonathan Sherratt [88] offers a distinctly different explanation of Type I diversity from either the incomplete-competition or fungiform-invasion hypotheses. Their model is a spatially explicit description of macrophage-tumor interactions that includes dynamics of a chemical regulator secreted by cancer cells that both attracts and activates macrophages. Macrophages are seen as able to bind to parenchyma cells to form a parenchyma-macrophage complex. Such complexes then fall apart, yielding an intact macrophage and unmodeled debris. If we let

$$\begin{aligned} l(\mathbf{x},t) &= \text{macrophage density at spatial point } \mathbf{x} \text{ at time } t,\\ m(\mathbf{x},t) &= \text{cancer (parenchyma) cell density},\\ n(\mathbf{x},t) &= \text{healthy cell density},\\ f(\mathbf{x},t) &= \text{concentration of the chemical regulator, and}\\ c(\mathbf{x},t) &= \text{parenchyma cell-macrophage complex density,} \end{aligned}$$

then the following is a nondimensional version of Owen and Sherratt's model:

$$\begin{cases} \dfrac{\partial l}{\partial t} = D_l\nabla^2 l - \chi_l\nabla(l\nabla f) + \dfrac{\alpha f l(N+1)}{N+l+m+n} + I(1+\sigma f) \\ \qquad\qquad -k_1 flm + k_2 c - \delta_l l, \\ \dfrac{\partial m}{\partial t} = D_m\nabla^2 m + \dfrac{\xi m(N+1)}{N+l+m+n} - m - k_1 flm, \\ \dfrac{\partial n}{\partial t} = D_n\nabla^2 m + \dfrac{n(N+1)}{N+l+m+n} - n, \\ \dfrac{\partial f}{\partial t} = D_f\nabla^2 f + \beta m - \delta_f f, \\ \dfrac{\partial c}{\partial t} = D_c\nabla^2 c + k_1 flm - k_2 c - \delta_c c. \end{cases} \tag{26}$$

Everything in this model moves about by simple diffusion with diffusion constants D_i, $i \in \{l, m, n, f, c\}$, and macrophages tend to migrate up the chemical regulator gradient with basic motility χ_l. All cell proliferation terms have the form

$$\frac{\psi(N+1)}{N+l+m+n}, \tag{27}$$

with ψ some simple function of assorted dependent variables and N a parameter that describes sensitivity of cells to crowding. The healthy cell population reaches equilibrium whenever $l+m+n=1$ in the absence of diffusion. Therefore, the variables are scaled such that when total cell density is unity, a sort of "carrying capacity" for healthy cells is reached. Note that in this model crowding inhibits only proliferation, not mortality. The remaining parameters include the rates at which macrophages proliferate in response to the chemical regulator (α), macrophages leave blood vessels to enter the tumor interstitium (I), blood-borne macrophages enter the tumor interstitium in response to the chemical regulator (σ), the macrophage-tumor cell complex forms (k_1) and dissociates (k_2), free macrophages disappear (δ_l), the chemical regulator is secreted by cancer cells (β), the chemical regulator decays (δ_c), and macrophage-cancer cell complexes dissociate. Finally, $\xi > 1$ measures the proliferative advantage cancer cells enjoy over healthy cells.

If one simplifies this model by turning chemotaxis off ($\chi_l = 0$), then numerical investigation reveals two interesting regimes. The first represents a smooth wavefront of cancer tissue infiltrating and completely eliminating surrounding healthy

cells. In this regime, the wave speed is approximately $2[D_m(\xi - 1)]^{\frac{1}{2}}$ per time, to first order. Their parameter estimates applied to this formula indicate that a 1 mm diameter tumor would take on the order of 100 days to grow.

The second regime is dynamically more surprising and shows the potential importance of immune attack on Type I diversity within a tumor. If the chemical regulator diffuses sufficiently well (D_f is large enough), then behind the invasion front a Turing pattern of alternating regions of high and low cancer cell density develops. In one dimension, the healthy cell density becomes very ragged as it decays outward in a pattern reminiscent of actual cancerous lesions. These patterns form because local areas in which cancer cell density, and therefore chemical regulator production, is high cause a sharp chemical gradient to form. Since both the gradient and diffusion constant are large, most of the chemical regulator moves out of areas of high cancer cell density. As a result, macrophages, following the chemical regulator, tend to cluster in areas of relatively low cancer cell density. Since these areas contain very few cancer cells, and therefore produce very little chemical regulator of their own, the gradient is maintained as long as the chemical regulator decay rate is sufficiently high. These patterns were observed in both one- and two-dimensional solutions.

Allowing macrophages to migrate up the chemical regulator gradient (allowing $\chi_l > 0$) stabilizes these Turing patterns in the following sense: chemotaxis tends to increase the critical value of D_f above which these patterns form. However, chemotaxis also appears to favor even wilder behavior once D_f gets high enough. The pattern following the invasion wavefront, which before was more or less regularly repeating regions of high and low cancer cell density, can become highly irregular, exhibiting the mixed histology often characteristic of malignant neoplasia.

4.2. **Causes of Type II diversity.** As already mentioned, diversity within malignant neoplasms is not limited to differences between parenchyma and a few "healthy" cell types. Even among parenchyma, cellular pleomorphism is a common feature, although it varies among tumors and even within the same tumor over time, typically declining as the tumor ages [68]. The question I now address is, how does cellular pleomorphism arise? At least three hypotheses exist. First, as already discussed, a number of different aspects of the intratumoral environment—nutrient concentration, hydrostatic and mechanical pressure, among other things—vary both temporally and spatially. Since cells are physiologically plastic, they can change their behavior and even form to accommodate the demands of their local environment. Therefore, pleomorphism may represent nothing more than accommodation of cells to different environmental conditions. We have already seen an example of this idea in the quiescent layer of some multicell spheroids. Despite the elegance of this hypothesis, it has rarely been evoked in any mathematical treatment to explain parenchyma pleomorphism beyond quiescence.

The cause of this neglect is probably the existence of an alternative hypothesis that, in this age of genomics, is more intuitively satisfying. Parenchyma cells have long been known to exhibit striking genetic variation, which was later discovered to be caused in part by dysfunction of their DNA-maintenance machinery [69, 78]. From this observation an explanation of cancer cell variation almost immediately follows—pleomorphism is driven by genetic polymorphism caused by the rapid accumulation of mutations among cancer cells. This hypothesis has been applied directly to explain variations in proliferation rate, invasion and metastasis potential, anaplasia (lack of differentiation), and senescence, in addition to cellular and

nuclear anatomy (reviewed in [18, 19]), although rarely has it been used in the mathematical oncology literature (see [103] for an exception).

The third hypothesis is really an extension of this genetic polymorphism idea. This new hypothesis, however, suggests that the history of mutations among cancer cells, while important, is still insufficient to explain the pattern of pleomorphism within any given tumor. One must also know how natural selection then sifted through the mutations to understand fully the diversity and frequency of parenchyma cell phenotypes. The role that natural selection plays depends critically on the functional nature of the pleomorphism. That is, are tumors integrated tissues, with a variety of cell types working together for their mutual benefit? Or are tumors a collection of uncooperative cell types competing for scarce resources? If the latter, then pleomorphism is a manifestation of niche segregation, and damaging or removing one cell type should have little effect on overall tumor growth. If the former, then pleomorphism is an adaptation of the tumor to the host; destruction of one subpopulation will cause disproportionate damage as the disruption of integrated function will ripple throughout the tumor.

Although the idea that natural selection acts within tumors is old [83, 87] and presented dogmatically in standard texts, the magnitude of selection's impact still demands evaluation. For example, if mutation rates are very high and environmental conditions extremely spatially and temporally variable, no consistent selection pressures will exist, thereby minimizing natural selection's role. Therefore, one should maintain natural selection and genetic polymorphism as distinct hypotheses.

For the remainder of this section I focus on the natural-selection hypothesis and ask, what traits does selection favor in the competition among parenchyma cell types? Certainly growth rate is an obvious candidate, but others have also been proposed, including efficient nutrient use and decreased dependence on oxygen. Below I review models of each of these suggestions.

4.2.1. *Natural selection favoring proliferation rate and efficient nutrient use.* As with Type I diversity, the earliest models of pleomorphism, by Seth Michelson et al. [75], grew from the Lotka-Volterra competition models. However, unlike Gatenby, Michelson et al. interpret the species as two different strains of cancer cells within a single tumor. In essence, the model "begins" after mutation has already created a challenger to the resident parenchyma strain. The question then is, will one strain eventually dominate or will a polymorphism result? In one variation, for example, Michelson et al. (see also Michelson and Leith [74]) allow one cell type to mutate into the other. In this model they represent the population sizes of the two cell strains as x and y and define the following model:

$$\begin{cases} \dfrac{\mathrm{d}x}{\mathrm{d}t} &= r_1 x\left(1-\dfrac{x}{K_1}-\lambda_1 y\right)-px, \\ \dfrac{\mathrm{d}y}{\mathrm{d}t} &= r_2 y\left(1-\dfrac{y}{K_2}-\lambda_2 x\right)+px, \end{cases} \tag{28}$$

with r_i and K_i the intrinsic rate of increase and carrying capacity, respectively, of cell type i; λ_i the effect of competition on strain i; and p the rate at which cell type 1 mutates into cell type 2. This model can have three fixed points: the origin, the point $(0, K_2)$, and a point in the interior representing a polymorphism. The authors use Dulac's criteria to show that no relevant limit cycles exist. The origin is never asymptotically stable if one assumes both $r_i > 0$; so, the dynamics are (almost

always) well characterized. In short, if $p > r_1(1 - \lambda_1 K_2)$, then solutions always approach the boundary fixed point, representing a monomorphic y-type population. If the inequality is reversed, the population approaches a well-characterized polymorphism asymptotically. So, if the x-type population suffers either a low intrinsic reproductive rate or high mortality, then selection will favor its complete annihilation. We can also see in this model selection punishing cells that use nutrients or space inefficiently—if y-type cells are inefficient, manifested as a limited "carrying capacity" (K_2 small), then x-type cells are less likely to be completely excluded.

A more sophisticated extension to these simple competition models provided by Gatenby and Thomas Vincent [45] can be used to predict how tumor populations are likely to evolve in the face of competition for resources, in this case glucose. Consider a tumor that contains one healthy cell population and $p-1$ subpopulations of parenchyma cell types. The number of healthy cells at time t is denoted $N_1(t)$, while $N_i(t)$, $i \in \{2, \ldots, p\}$, represents the size of the ith cancer subpopulation. Cells of all types take up and metabolize glucose, the absolute amount of which is denoted $R(t)$. Gatenby and Vincent then write the following model to represent competition for glucose within this heterogeneous tumor:

$$\begin{cases} \dfrac{\mathrm{d}N_1}{\mathrm{d}t} &= \alpha_n \left(1 - \dfrac{N_1}{K_n}\right) \left(\dfrac{E_n R^2}{R_n^2 + R^2} - m_n\right) N_1, \\ \dfrac{\mathrm{d}N_i}{\mathrm{d}t} &= \alpha_c \left(1 - \dfrac{S}{K_i}\right) \left(\dfrac{E_i R^2}{R_c^2 + R^2} - m_c\right) N_i, \quad i \in \{2, \ldots, p\}, \\ \dfrac{\mathrm{d}R}{\mathrm{d}t} &= r - \dfrac{E_n R^2}{R_n^2 + R^2} N_1 - \displaystyle\sum_{i=2}^{p} \dfrac{E_i R^2}{R_c^2 + R^2} N_i, \\ r &= r_e(m_n N_1 + m_c S), \\ S &= \displaystyle\sum_{i=2}^{p} N_i, \end{cases} \tag{29}$$

where α_n and α_c are intrinsic rates of increase for healthy and cancer cells (invariant across strains), respectively; K_i and E_i, $i \in \{1, \ldots, p\}$, are "carrying capacities" and maximum substrate uptake rates for all cell types, respectively; R_n and R_c measure the sensitivity of nutrient uptake to changes in nutrient concentration, and m_n and m_c represent glucose oxidized for purposes other than proliferation, which one can think of as maintenance metabolism. The function r represents glucose delivery through the blood, which increases with tumor size. Gatenby and Vincent appear to assume that microvessel density varies in proportion to glucose demand for maintenance metabolism, so they modify the basic glucose delivery rate, r_e, by the weighted average of basic glucose demand.

In this model the parameters assumed to be under selection are K and E and are considered to be random variables. They assume that normal cells' carrying capacities and basic nutrient uptake rates distribute normally around means μ_K and μ_E, with variance σ_n^2 for both distributions. Similarly, parameter values for cancer cells are normally distributed with means ν_K and ν_E and variance σ_c for both. To determine how the population evolves, Gatenby and Vincent exploit a method involving fitness-generating functions that essentially allows them to write an expression for the fitness of all possible cell types for any given population composition. With this adaptive landscape, they can then write a differential equation

for the change in population size for any strategy in any population. With such an equation one can find evolutionary equilibria, equivalent to evolutionary stable strategies [46, 73], by finding the population configuration at which the fitnesses of all cell types are zero.

The results of this model suggest that when cancer arises, glucose concentration tends to decline, because the basic metabolic rate of the tissue (tumor) increases. Because glucose becomes scarce, natural selection favors cells that can sequester and metabolize glucose efficiently (maximize both K and E). So over time the tumor is able to maintain its proliferation rate in the face of fierce competition for glucose. In addition, this model is among the first to reproduce the observed decline in tumor pleomorphism as tumors progress.

Further support for the hypothesis that selection favors efficient nutrient use comes from a model by Yang Kuang et al. [60]. In this model we imagine a tumor growing in an organ with mass $x(t)$. The tumor contains two different parenchyma cell types with masses $y_1(t)$ and $y_2(t)$. Nutrient is delivered to the cells through a dynamic vascular network with a total mass of vascular endothelial cells (VECs) of $z(t)$. Total tumor phosphorus is denoted by P and is partitioned into five different compartments: the interstitial fluid, healthy cells, cells of the first parenchyma type, cells of the second parenchyma type, and VECs. Each unit mass of healthy cells, including VECs, contains n units of phosphorus, while parenchyma cells of type 1 and type 2 hold m_1 and m_2 units, respectively. Therefore, if we denote extracellular phosphorus as P_e, then $P_e = P - [n(x+z) + m_1 y_1 + m_2 y_2]$. With this notation, Kuang et al. suggest the following model:

$$\begin{cases} \dfrac{\mathrm{d}x}{\mathrm{d}t} &= x\left(a\min\left(1, \dfrac{P_e}{fnk_h}\right) - d_x - (a-d_x)\dfrac{x+y_1+y_2+z}{k_h}\right), \\ \dfrac{\mathrm{d}y_1}{\mathrm{d}t} &= y_1\left(b_1\min\left(1, \dfrac{\beta_1 P_e}{fm_1k_h}\right)\min(1,L) - d_1 - (b_1-d_1)\dfrac{y_1+y_2+z}{k_t}\right), \\ \dfrac{\mathrm{d}y_2}{\mathrm{d}t} &= y_2\left(b_2\min\left(1, \dfrac{\beta_2 P_e}{fm_2k_h}\right)\min(1,L) - d_2 - (b_2-d_2)\dfrac{y_1+y_2+z}{k_t}\right), \\ \dfrac{\mathrm{d}z}{\mathrm{d}t} &= c\min\left(1, \dfrac{P_e}{fnk_h}\right)(y_1(t-\tau)+y_2(t-\tau)) - d_z z, \end{cases} \tag{30}$$

where $L = g(z - \alpha(y_1+y_2))(y_1+y_2)$, a, b_1, b_2, and c represent intrinsic rates of increase of all cell types; all terms d_i are basic death rates; k_h and k_t represent limiting sizes for the healthy organ and tumor, respectively; f is the intracellular fluid fraction; and L is a measure of vascular supply. In particular, α represents the mass of tumor cells one unit of blood vessels can just barely maintain, and g measures sensitivity of tumor tissue to lack of blood. Also, Kuang et al. assume that tumor tissue starved for blood releases an angiogenic signal. This signal is distilled by VECs from a complex mix of pro- and antiangiogenic chemical growth factors released by all cells in the tumor. Upon receipt of the signal, VECs respond by reproducing, moving toward the blood-starved region and forming new microvessels. Kuang et al. further assume that the VEC response is delayed by τ time units, representing the time needed for cells to transduce and respond to the chemical signal and complete their reproductive, motility, and differentiation

programs. Finally, parameters β_i represent the effect of a drug able to modulate, generally inhibit, cell type i's ability to sequester phosphorus from the interstitium.

Model (30) admits two possible limiting factors: blood supply and phosphorus. However, simulations with reasonably realistic parameter values suggest that phosphorus is the key limiting factor, determining both growth rate and final tumor mass. In this case, then, what type of cell does natural selection favor—cells with a high or low phosphorus requirement (high or low m_i)? The nutrient-use efficiency hypothesis suggests that selection will favor the most efficient type; that is, the type that minimizes m_i. However, the reality is complicated by the fact that phosphorus use relates to growth rate [34, 60, 101] in the following way. Cells require phosphorus primarily for nucleic acid, and rapidly proliferating cancer cells must synthesize large amounts of nucleic acids, primarily in the form of ribosomes [101], to build proteins needed for cell division. In fact the number of ribosomes in cancer cells appears to correlate with cancer aggressiveness (reviewed in [34]). Therefore, selection for the aggressive cell type can work directly against selection for efficient nutrient use.

Model (30) suggests that selection's choice between nutrient-use efficiency and aggressive proliferation depends on the state of the tumor. In particular, when tumors are small and well supplied with phosphorus and blood, the more aggressively proliferating cell type may have the advantage, growing faster than its less aggressive competitor. However, as the tumor approaches its asymptotic limit, competition for phosphorus increases as it becomes limiting. Then selection changes favor and gives the advantage to the more efficient type, which eventually drives the aggressive phenotype to extinction (Fig. 4). Therefore, this model predicts that as tumors age they become less aggressive and more miserly with nutrients.

4.2.2. *Natural selection favoring insensitivity to hypoxia.* As already discussed (section 3.4), malignant tumors and their peritumoral environments tend to be relatively acidic, probably because tumor cells favor glycolysis and fermentation over the tricarboxilic acid cycle. Gatenby and his colleagues [43, 45, 97] suggest that natural selection provides the answer as to why. Carcinomas by definition begin within epithelial tissue. This tissue is defined by the presence of a basement membrane upon which the epithelial cells live (Fig. 5). Usually the vasculature servicing such tissue lies on the opposite side of the basement membrane; therefore, premalignant carcinoma precursors, which by definition cannot penetrate the basement membrane, are constrained to expand away from the blood supply. (Such geometry raises doubts about the validity of tumor cell spheroids as models of nascent carcinoma.) Cells in such a situation able to produce ATP under hypoxic conditions will then be favored. Since these geometrical constraints apply to essentially all carcinomas, selection favoring glycolytic oxidation of glucose will be nearly ubiquitous [43, 45, 97].

Two recent models [39, 106] connect this hypothesis with molecular biology of cancer cells through the tumor suppressor gene *p53*, whose product, p53, the editors of *Science* declared "molecule of the year" in 1993. Among its many demonstrated functions, *p53*'s product activates the apoptosis mechanism in "stressed" cells. One form of stress to which p53 appears to respond is hypoxia. Evidence for this conclusion comes from studies of *p53*-deficient cells in culture, which commit apoptosis less frequently than intact wild-type cells in hypoxic environments [47, 99]. This observation is profoundly significant to cancer biologists, because *p53* is widely regarded as the most commonly disrupted gene among cancers as a whole,

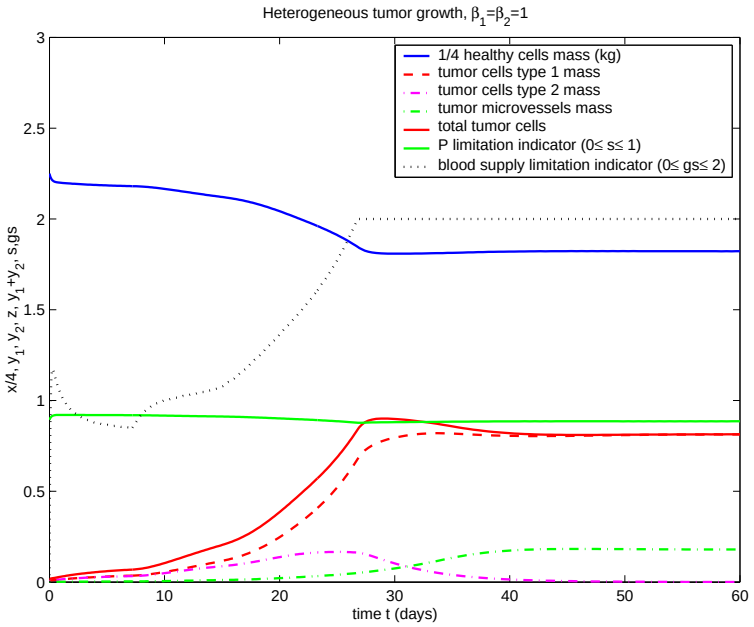

FIGURE 4. A numerical solution to model (30) with $a = 3$, $m_1 = 20$, $m_2 = 22$, $n = 10$, $k_t = 3$, $f = 0.6667$, $P = 150$, $\alpha = 0.05$, $b_1 = 6$, $b_2 = 6.6$, $\tau = 7$, $d_x = 1$, $d_z = 0.2$, $d_1 = 1$, $d_2 = 1$, $g = 100$, and $[x(0), y_1(0), y_2(0), z(0)] = [9, 0.01, 0.01, 0.001]$. This example shows that selection appears to favor neither cell type until phosphorus becomes limiting. From [60, p.233]

mutated in over 50% of all malignant neoplasms, and many cancerous tumors suffer regions of local hypoxia (see section 3.5). If selection frequently favors cancer cells able to withstand hypoxia as Gatenby and colleagues have suggested, perhaps *p53* disruption is a common mechanism, along with other metabolic changes, by which cells acquire the favored trait. Empirical support for this interpretation comes from observations of cell populations evolving a dysfunctional *p53* gene when exposed to hypoxic environments [79].

Selection for dysfunctional *p53* was studied quantitatively by David Gammack et al. [39]. Building on the earlier model of Kevin Thompson and Janice Royds [106], Gammack et al. model the dynamics of three quantities: the number of tumor cells with the wild-type (normal) *p53* gene ($N(t)$), the number of tumor cells with the mutated *p53* gene ($M(t)$), and molecular oxygen concentration ($C(t)$). Tumor cells of both types consume molecular oxygen, proliferate, and die at rates dependent on O_2 concentration. Oxygen is supplied to cells in one of two ways, depending on whether the model represents cells in culture in some virtual experiment or an in vivo tumor. In the in vitro situation, O_2 is supplied exogenously in the media. We imagine the researchers of this virtual experiment varying the O_2 concentration in the following way: for a period of length δ, oxygen is maintained at physiologically normal levels (normoxia); then a period of hypoxia that lasts for τ time units follows. We imagine that the researchers control δ and τ and repeat the procedure some number of times. In the model of an in vivo tumor, cells can also be exposed

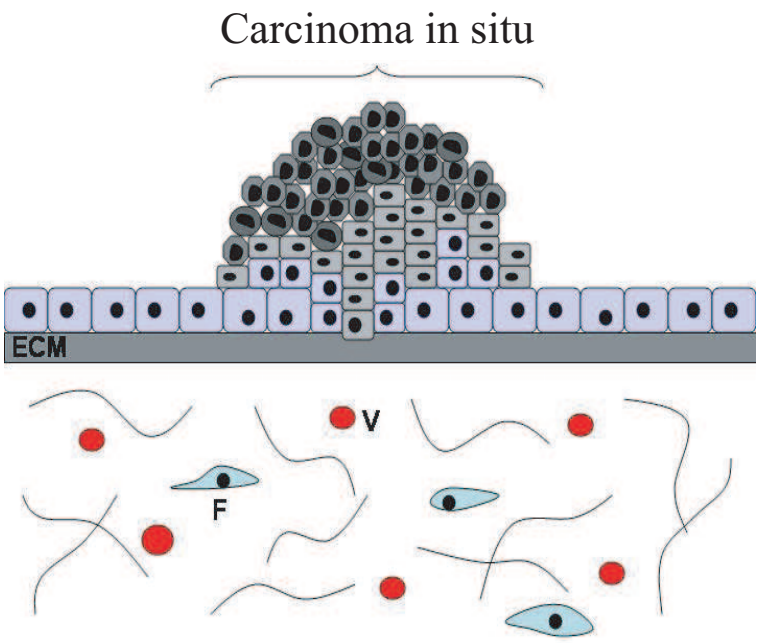

FIGURE 5. Illustration of nascent carcinoma in situ in a simple epithelium. ECM refers to the basement membrane constructed of extracellular matrix. Red circles labelled 'V' represent blood vessels, and cells labelled 'F' are fibroblasts in the underlying mesenchyme.

to repeated rounds of normoxia and hypoxia but only if blood vessels collapse from internal pressures (see section 3.5.1). This collapse occurs whenever total cell numbers reach a prescribed threshold, N^*. Once $N + M = N^*$, hypoxia begins for a fixed period of time, τ, representing the time required for angiogenesis to reconstruct a sufficient vascular infrastructure.

From these assumptions, Gammack et al. build the following model:

$$\begin{cases} \dfrac{\mathrm{d}N}{\mathrm{d}t} &= \dfrac{A_N C^p}{C_{N_1}^p + C^p} N - B_N \left(1 - \dfrac{\sigma_N C^q}{C_{N_2}^q + C^q}\right) N(N+M), \\ \dfrac{\mathrm{d}M}{\mathrm{d}t} &= \dfrac{A_M C^p}{C_{M_1}^p + C^p} M - B_M \left(1 - \dfrac{\sigma_M C^q}{C_{M_2}^q + C^q}\right) M(N+M), \\ \dfrac{\mathrm{d}C}{\mathrm{d}t} &= \lambda C_{ex}(t) - \Gamma_N \dfrac{A_N C^p}{C_{N_1}^p + C^p} N - \Gamma_M \dfrac{A_M C^p}{C_{M_1}^p + C^p} M - \Gamma_C C. \end{cases} \tag{31}$$

Parameters A_i and B_i represent maximum proliferation and mortality rates of cell type i, respectively; $C_{N_1}^p$ and $C_{M_1}^p$ measure how sensitive each cell type's reproductive response is to changes in O_2 concentration. Similarly, $C_{N_2}^p$ and $C_{M_2}^p$ measure how sensitive mortality rates are to changes in O_2 concentration. Both p and q are free parameters with no obvious physiological meaning but may be required to fit the model to data. Parameters σ_N and σ_M can be interpreted as a measure of basal mortality that occurs even in a perfect environment; that is, as the O_2 concentration

Table 1. Evolutionary payoff matrix for the model by Bach et al. [11]

Neighborhood	A+	A−
A+, A−	$1-i-j$	$1+j$
A+, A−	$1-i-j$	1
A−, A−	$1-i$	1

NOTE: Strain A+ secretes an angiogenesis factor, whereas strain A− does not. Adapted from [11].

gets large, mortality asymptotes at $B_i(1-\sigma_i)$. However, actual estimates of σ from cell culture data reviewed by Gammack et al. put it very close to unity for both wild-type and *p53*-deficient cell lines, indicating that mortality in these assays was negligible when O_2 concentration was high. The function $\lambda C_{ex}(t)$ represents the rate at which O_2 is supplied to the system as described in the previous paragraph. Oxygen is consumed by cells at base rates Γ_i for cell type $i \in \{N, M\}$, and total O_2 consumption depends on the growth rate of each cell type. Finally, O_2 diffuses out of the system or is consumed by other processes at linear rate Γ_C.

Data from Thompson and Royds [106] indicate that wild-type and *p53*-deficient cell lines differ mostly in basic mortality rates and sensitivity to O_2. Roughly speaking, wild-type cells have a larger basic mortality rate ($B_N > B_M$) and suffer more from hypoxia ($C_{N_1} > C_{M_1}$ and $C_{N_2} > C_{M_2}$). Not surprisingly, *p53*-deficient cells tend to outcompete wild-type cells in the virtual experiment. In one run, for example, with an initial cell culture in which wild-type cells outnumbered *p53*-deficient mutants by orders of magnitude and periods of normoxia were only slightly longer than hypoxic periods, mutants became the dominant cell type between the fourth and fifth hypoxic episode. Of course, the length of time it takes for mutants to become dominant depends strongly on how long hypoxic and normoxic periods last. In general, Gammack et al. found that longer periods of hypoxia slowed mutant invasion, and longer periods of normoxia speeds mutant invasion. Higher oxygen concentrations during normoxic episodes also favor invasion. In contrast to the nutrient-use efficiency hypothesis presented in section 4.2.1, changes in the rate at which mutant cells consume oxygen, Γ_M, had very little effect; however, increasing oxygen consumption by mutant cells very slightly decreased the invasion rate, as predicted by the nutrient-use hypothesis.

Results of the in vivo case were similar. Once again, under the estimated parameters, *p53*-deficient mutants tended to invade tumors in which they were initially rare, whether solutions permitted oscillations or not. Oscillatory solutions like those in the in vitro case arose when the oxygen concentration during normoxic episodes was sufficiently high, and the rate at which mutants consumed O_2 was sufficiently low. Once again, variations in Γ_M hardly affected the mutant invasion rate, which was once again driven primarily by the duration of the hypoxic episode.

5. **Synthesis: Competition, natural selection and necrosis.** Before leaving the topic of natural selection's role in malignant neoplasia, it is necessary to ask, are there any direct theoretical explorations of niche segregation as a cause of cellular diversity in tumors? Although this question is at the heart of the selection hypothesis of cellular pleomorphism, very few studies that deal with it directly have been published. Among those that have is a game-theory model by Lars Bach et al. [11]. This model, based on earlier work by Ian Tomlinson and Walter Bodmer

[109, 108], assumes that two different strains of parenchyma cells exist within the tumor. One strain, denoted by A+, secretes some chemical that is beneficial to the cells in its neighborhood—say, an angiogenesis signal. The other strain, A−, does not. Otherwise, all cells are identical. In Bach et al.'s model, neighborhoods consist of three cells. If only one cell in the neighborhood secretes the chemical, then the group gains no benefit, because, it is assumed, the chemical concentration remains too small to elicit the effect. However, if at least two of the three cells secrete the chemical, then all three enjoy an increased reproductive output of j units above normal. On the down side, there is a cost associated with making the chemical; those that do suffer a deduction of i to their expected reproductive output. These considerations lead to the evolutionary payoff matrix shown in Table 1.

A discrete-time dynamical system model of these payoffs shows that selection can allow coexistence of both strains under certain circumstances. However, niche segregation cannot explain this behavior, for the following reason. If a tumor starts with "cooperators" that secrete the angiogenesis factor and is later invaded by a mutant "defector" strain that does not, then both defector and cooperator populations can persist. However, if the roles of resident and potential invader are reversed—that is, a population of defectors is challenged by cooperators—the cooperators die out, leaving a monomorphic defector population. One can interpret these results biologically as follows: defectors can invade a tumor full of cooperators as a sort of parasite living off of the cooperator's ability to bring in resources; however, cooperators are always hurt by the presence of defectors. Therefore, polymorphism can be explained as parasitism instead of niche segregation.

This conclusion was corroborated in a study I conducted of a model with two competing parenchyma strains that differ in their abilities to secrete angiogenesis signals. However, unlike the Bach et al. model, this one allows dynamic population sizes and a broader array of potential differences among cell types. Similar in construction to models by Zvia Agur, Levon Arakelyan and their colleagues [2, 9], my model tracks the mass of two strains of parenchyma cells, denoted by $x_1(t)$ and $x_2(t)$. In addition, the model also follows the total mass of immature VECs from which mature microvessels are made, $y(t)$, and the total length of microvessels within the tumor, $z(t)$. With this notation, the model becomes

$$\begin{cases} \dfrac{dx_1}{dt} &= \Phi_1(v)x_1, \\ \dfrac{dx_2}{dt} &= \Phi_2(v)x_2, \\ \dfrac{dy}{dt} &= (\alpha H(x_1, x_2, z) - \beta)\, y, \\ \dfrac{dz}{dt} &= \gamma y - \delta v z, \end{cases} \tag{32}$$

where $v(t) = z/(x_1 + x_2)$, $H(x_1, x_2, z) = (x_1 h_1(v) + x_2 h_2(v))/(x_1 + x_2)$, Φ_i represents per-capita growth functions for both types of parenchyma, α is the rate at which immature VECs convert the angiogenesis signal into growth, H is the mean angiogenesis secretion rate within the tumor, h_i is the per-capita angiogenesis secretion rate for cell type i, β expresses both the VEC death and maturation rates, γ represents the rate at which maturing VECs convert themselves into new blood vessels, and δ is the base rate at which blood vessels are broken down during remodeling. In numerical analysis, the functions Φ take a form similar to that of cell

growth in model (31) without the crowding term; that is,

$$\Phi_i(v) = \frac{A_i C(v)^{p_i}}{\hat{c}_{i1}^{p_i} + C(v)^{p_i}} - B_i \left(1 - \frac{\sigma_i C(v)^{q_i}}{\hat{c}_{i2}^{q_i} + C(v)^{q_i}}\right), \tag{33}$$

where $C(v)$ is the oxygen pressure and all other parameters equate to their analogues in model (31). The cell type-specific angiogenesis secretion rate obeys a function like the following:

$$h_i(v) = r_i C(v) e^{-\xi_i C(v)}, \tag{34}$$

where r_i measures a type i cell's commitment to producing the angiogenesis signal and ξ_i expresses how sensitive this commitment is to changes in local oxygen pressure.

This model supports the hypothesis that natural selection favors aggressively proliferating cell types, at least early in tumor growth, but with a twist. Work in preparation shows that if strains differ only in their basic proliferation rates such that $A_1 > A_2$, strain 1 always ends up dominating the tumor regardless of initial conditions. In fact, one can show that for a broad array of forms for the growth functions Φ, aggressively proliferating cell types are always favored. However, a tumor invaded by a more aggressive strain may end up *clinically* less aggressive. This paradox arises when the invading, aggressive cell type is sufficiently inept at producing the angiogenesis signal. Natural selection is blind to angiogenesis secretion and so always favors the aggressive invader. But because the favored strain cannot entice new blood vessels to grow very well, the tumor eventually ends up with a lower microvessel density and is therefore relatively hypoxic. In certain circumstances, this hypoxia can become so profound that the tumor regresses. One can describe such circumstances as a hypertumor—one tumor invading and destroying part of an existing tumor. And once again we see competition resulting in something akin to parasitism.

This hypertumor phenomenon hands us yet another hypothesis explaining necrosis. Superficially, one can view it as a variant of the nutrient-limitation hypothesis. However, certain predictions distinguish it from the other ideas. In particular, one will recognize a hypertumor not just as regions of nutrient deficiency but as regions of nutrient deficiency that always correlate with invading cells displaying cytological or genetic features of aggressive proliferation.

6. **Conclusion.** Perhaps the most obvious conclusion one can draw from this review is that existing mathematical theory provides significant insight into the causes of the three phenomena studied—necrosis, total cell diversity, and cellular pleomorphism. Mathematical oncology provides a much richer theory than that underlying explanations of these phenomena in standard pathology texts or even the massive compendium edited by Vincent DeVita et al. [31]. In essence, these more clinical sources either treat necrosis and cell diversity as explained—necrosis occurs from nutrient deficiency with no further details, and pleomorphism results from natural selection, again with no more details—or ignore them altogether. But as existing literature makes clear, these phenomena are far from explained. For example, any of the following possible causes of necrosis remain viable hypotheses:

1. Nutrient deficiency, caused by
   a. the geometry of the tumor—spheroids, tumor cords, carcinoma in situ, and remote regions within a mature tumor;
   b. ischemia from vascular collapse;

   c. ischemia from heterogeneous blood flow and hematocrit distributions in existing vascular nets;
   d. hypertumor
2. Local acidosis from tumor cell acid secretion
3. Mechanical disruption of cells from pressures within the tumor

Of course, these models cannot distinguish which is or are correct; only empirical study can do that. However, many of the models presented in this review make testable predictions or at the least point to refinements from which testable predictions can be deduced.

Similar conclusions can be made for the other phenomena. In particular, mathematical oncology has identified at least the following possible causes of total cell diversity in malignant neoplasms:

1. Incomplete competitive exclusion
2. Fungiform invasion
3. Turing patterns

In addition, potential explanations of cellular pleomorphism include

1. anatomical and physiological accommodation to spatially and temporally varying environments;
2. mutation;
3. mutation followed by natural selection leading to
   a. niche segregation
   b. tissue-like integration.

The favored hypothesis of natural selection leads us to ask what traits selection will tend to favor. Once again, mathematical oncology provides a variety of hypotheses:

1. Aggressive proliferation
2. Efficient use of scarce nutrients
3. Insensitivity to hypoxia
4. Some combination of the three

And, as with necrosis, insight gained from most of these models provides a basis for practical predictions that can be tested in the lab or clinic.

Unfortunately most of these insights have gone largely unexploited by the empirical cancer biology community. To see this in a very profound way, compare the literature-cited sections of the basic cancer biology chapters in [31] and the historical review of mathematical oncology in [10]. The former is a compendium of modern cancer biology from a pathologist's or clinician's standpoint, and the latter is an outstanding review of the major themes in mathematical oncology. Despite their focus on the same disease, these two sources share very few citations, especially theory papers. In essence, neither group is aware of the other's literature.

Trying to establish why mathematical oncology has influenced the work of experimentalists and medical doctors so lightly is dangerous business, but ignoring it is even more dangerous. One possibility, perhaps the most obvious, may be that the two groups by and large cannot communicate because they speak different technical languages, and translators are rare. Hopefully this situation is changing as more students seek training in both advanced molecular biology and mathematics. Nevertheless, despite its obvious appeal, this explanation cannot be the only reason for the disconnect, because although rare, very talented translators have always existed between the empirical and theoretical communities.

Another contributing factor to the lack of knowledge transfer may also be the wildly different research focuses of the two groups. As discussed in the introduction, empirical cancer biologists tend to focus on the molecular biology of cancer cells, as is obvious from a casual inspection of any empirical cancer journal. Mathematical oncologists, on the other hand, tend to focus on aspects of tumor ecology like those reviewed here, plus immune predation, the effects of cytotoxic chemotherapy and radiation therapy on competition among parenchyma cells, and other aspects of tumor ecology. So, the outlook, interests, and research tools characteristic of experimentalists and theoreticians have traditionally differed so much that there has been very little overlap in research programs. Again, a look through DeVita et al. [31] makes clear that the practice of oncology would hardly be changed if no one had ever written a mathematical model of cancer.

The question then becomes, where, if anywhere, will empirical and mathematical oncology meet? In particular, how best can mathematical oncology serve experimentalists by helping direct their work in the lab and clinic? Certainly the insights gained so far by mathematical oncology should not be abandoned, and work on specific systems, especially drug trials on cell cultures and angiogenesis inhibition, along with other recent collaborations between empiricists and theoreticians, are already building common interests. However, one major question of growing importance appears to be a perfect place where the interests and tools of molecular biologists, experimental cell biologists, and mathematical biologists meet. That question is, how exactly do parenchyma, stroma—including ECM and stromal cells— and immune and peritumoral cells interact to promote malignancy? This question obviously involves molecular and cellular biology. Genes for growth factors like the various forms of VEGF, their receptors, such as flt-1, matrix metalloproteinases, and a host of other molecules, choreograph all interactions among all cell types and even nonliving elements within malignant and premalignant tumors. But these interactions are primarily ecological in nature, ultimately determining the outcome of competition, cooperation, and predation. Mathematical oncologists can attack this problem with extensions of formalisms already in place, like multicell spheroids with mixtures of cell types currently under investigation by empiricists [78]. More important, mathematical oncologists must begin adopting formalisms representative of more realistic geometries encountered in carcinoma (Figs. 1 and 5), especially when modeling nascent tumors. But, no matter how one attacks the problems posed by malignant neoplasia, the time has arrived to begin melding the molecular and evolutionary ecology approaches to cancer biology, and the mathematical oncology community has, above all others, the skill set to do it.

Acknowledgments. The micrograph in Figure 1 was taken with the kind help of Dr. Tim Crowley and the Arizona State University Bioengineering Visualization Laboratory. Dr. Dana Devine of Midwestern University in Glendale, Arizona, provided invaluable assistance in interpreting the pathology displayed in Figure 1. I am happy to thank Professor Yang Kuang for encouraging and reviewing this work. I also thank Craig Thalhauser, Dr. Bethel Nagy and Dr. Kim Cooper for their reviews and comments. This work was supported in part by the NSF and the NIH under grant no. DMS/NIGMS-0342388.

REFERENCES

[1] J. A. Adam, General aspects of modeling tumor growth and immune response, in A Survey of Models for Tumor-Immune System Dynamics, J. A. Adam and N. Bellomo, eds., Birkhäuser, Berlin, 1997, 15–87.

[2] Z. Agur, L. Arakelyan, P. Daugulis, and Y. Ginosar, Hopf point analysis for angiogenesis models, Disc. Cont. Dyn. Sys. B, 4 (2004), 29–38.

[3] T. Alarcón, H. M. Byrne, and P. K. Maini, A cellular automaton model for tumor growth in inhomogeneous environment, J. Theor. Biol., 225 (2003), 257–274.

[4] ———, Towards whole-organ modelling of tumour growth, Prog. Biophys. Mol. Biol., 85 (2004), 451–472.

[5] B. Alberts, D. Bray, J. Lewis, M. Raff, K. Roberts, and J. Watson, The Molecular Biology of the Cell, Garland, New York, 3rd ed., 1994.

[6] D. Ambrosi and F. Mollica, On the mechanics of a growing tumor, Int. J. Eng. Sci., 40 (2002), 1297–1316.

[7] ———, The role of stress in the growth of a multicell spheroid, J. Math. Biol., 48 (2004), 477–499.

[8] A. R. A. Anderson and M. A. J. Chaplain, Continuous and discrete mathematical models of tumor-induced angiogenesis, Bull. Math. Biol., 60 (1998), 857–900.

[9] L. Arakelyan, Y. Merbl, P. Daugulis, Y. Ginosar, V. Vainstein, V. Selitser, Y. Kogan, H. Harpak, and Z. Agur, Multi-scale analysis of angiogenic dynamics and therapy, in Cancer Modeling and Simulation, Preziosi, ed., Chapman and Hall/CRC, Boca Raton, FL, 2003, 185–219.

[10] R. P. Araujo and L. S. McElwain, A history of the study of solid tumor growth: The contribution of mathematical modelling, Bull. Math. Biol., 66 (2004), 1039–1091.

[11] L. A. Bach, S. M. Bentzen, J. Alsner, and F. B. Christiansen, An evolutionary-game model of tumor-cell interactions: Possible relevance to gene therapy, Eur. J. Cancer, 37 (2001), 2116–2120.

[12] M. H. Barcellos-Hoff and S. A. Ravani, Irradiated mammary gland stroma promotes the expression of tumorigenic potential by unirradiated epithelial cells, Cancer Res., 60 (2000), 1254–1260.

[13] A. Bertuzzi, A. D'Onofrio, A. Fasano, and A. Gandolfi, Regression and regrowth of tumour cords following single-dose anticancer treatment, Bull. Math. Biol., 65 (2003), 903–931.

[14] ———, Modelling cell populations with spatial structure: Steady state and treatment-induced evolution of tumor cords, Disc. Cont. Dyn. Sys. B, 4 (2004), 161–186.

[15] A. Bertuzzi, A. Fasano, A. Gandolfi, and D. Marangi, Cell kinetics in tumour cords studied by a model with variable cell cycle length, Math. Biosci., 177/178 (2002), 103–125.

[16] A. Bertuzzi and A. Gandolfi, Cell kinetics in a tumor cord, J. Theor. Biol., 204 (2000), 587–599.

[17] N. A. Bhowmick, E. G. Neilson, and H. L. Moses, Stromal fibroblasts in cancer initiation and progression, Nature, 432 (2004), 332–337.

[18] L. P. Bignold, The mutator phenotype theory can explain the complex morphology and behaviour of cancers, Cell. Mol. Life Sci., 59 (2002), 950–958.

[19] ———, The mutator phenotype theory of carcinogenesis and the complex histopathology of tumours: Support for the theory from the independent occurrence of nuclear abnormality, loss of specialization and invasiveness among occasional neoplastic lesions, Cell. Mol. Life Sci., 60 (2003), 883–891.

[20] S. Britto Garcia, M. Novelli, and N. A. Wright, The clonal origin and clonal evolution of epithelial tumours, Int. J. Exp. Pathol., 81 (2000), 89–116.

[21] A. C. Burton, Rate of growth of solid tumours as a problem of diffusion, Growth, 30 (1966), 157–176.

[22] H. M. Byrne, Modelling avascular tumor growth, in Cancer Modelling and Simulation, L. Preziosi, ed., Chapman and Hall/CRC, Boca Raton, FL., 2003.

[23] H. M. Byrne and M. A. J. Chaplain, Growth of nonnecrotic tumors in the presence and absence of inhibitors, Math. Biosci., 130 (1995), 151–181.

[24] ———, Growth of necrotic tumors in the presence and absence of inhibitors, Math. Biosci., 135 (1996), 187–216.
[25] M. A. J. Chaplain, Mathematical modelling of angiogenesis, J. Neurooncol., 50 (2000), 37–51.
[26] M. A. J. Chaplain and A. R. A. Anderson, Mathematical modelling of tumor invasion, in Cancer Modeling and Simulation, Preziosi, ed., Chapman and Hall/CRC, Boca Raton, FL, 2003, 269–297.
[27] C. Y. Chen, H. M. Byrne, and J. R. King, The influence of growth-induced stress from the surrounding medium on the development of multicell spheroids, J. Math. Biol., 43 (2001), 191–220.
[28] R. S. Cotran, V. Kumar, and T. Collins, Robbins' Pathologic Basis of Disease, W.B. Saunders, Philadelphia, 6th ed., 1999.
[29] V. Cristini, J. Lowengrub, and Q. Nie, Nonlinear simulation of tumor growth, J. Math. Biol., 46 (2003), 191–224.
[30] Y. Deugnier, Iron and liver cancer, Alcohol, 30 (2003), 145–150.
[31] V. T. DeVita, S. Hellman, and S. A. Rosenberg, eds., Cancer: Principles and Practice of Oncology, Lippencott-Raven, Philadelphia, 5th ed., 1997.
[32] O. De Wever and M. Mareel, Role of tissue stroma in cancer cell invasion, J. Pathol., 200 (2003), 429–447.
[33] J. Dyson, R. Villella-Bressan, and G. Webb, The steady state of a maturity structured tumor cord cell population, Disc. Cont. Dyn. Sys. B, 4 (2004), 115–134.
[34] J. J. Elser, J. D. Nagy, and Y. Kuang, Biological stoichiometry: An ecological perspective on tumor dynamics., Biosci., 53 (2003), 1112–1120.
[35] G. I. Evan and K. H. Vousden, Proliferation, cell cycle and apoptosis in cancer, Nature, 411 (2001), 342–348.
[36] J. Folkman, P. Hahnfeldt, and L. Hlatky, Cancer: Looking outside the genome, Nat. Rev. Mol. Cell. Biol., 1 (2000), 76–79.
[37] S. J. Franks, H. M. Byrne, J. R. King, J. C. E. Underwood, and C. E. Lewis, Modelling the early growth of ductal carcinoma in situ of the breast, J. Math. Biol., 47 (2003), 424–452.
[38] A. Friedman and F. Reitich, Analysis of a mathematical model for the growth of tumors, J. Math. Biol., 38 (1999), 262–284.
[39] D. Gammack, H. M. Byrne, and C. E. Lewis, Estimating the selective advantage of mutant p53 tumour cells to repeated rounds of hypoxia, Bull. Math. Biol., 63 (2001), 135–166.
[40] R. A. Gatenby, Models of tumor-host interaction as competing populations: Implications for tumor biology and treatment, J. Theor. Biol., 176 (1995), 447–455.
[41] R. A. Gatenby and E. T. Gawlinski, A reaction-diffusion model of cancer invasion, Cancer Res., 56 (1996), 5745–5753.
[42] R. A. Gatenby and E. T. Gawlinski, The glycolytic phenotype in carcinogenesis and tumor invasion: Insights through mathematical models, Cancer Res., 63 (2003), 3847–3854.
[43] R. A. Gatenby and R. J. Gillies, Why do cancers have high aerobic glycolysis?, Nature Rev. Cancer, 4 (2004), 891–899.
[44] R. A. Gatenby, P. K. Maini, and E. T. Gawlinski, Analysis of tumor as an inverse problem provides a novel theoretical framework for understanding tumor biology and therapy, Appl. Math. Lett., 15 (2002), 339–345.
[45] R. A. Gatenby and T. L. Vincent, An evolutionary model of carcinogenesis, Cancer Res., 63 (2003), 6212–6220.
[46] S. A. H. Geritz, E. Kisdi, G. Meszéna, and J. A. J. Metz, Evolutionarily singular strategies and the adaptive growth and branching of the evolutionary tree., Evol. Ecol., 12 (1998), 35–57.
[47] T. G. Graeber, C. Osmanian, T. Jacks, D. E. Housman, C. J. Koch, S. W. Lowe, and A. J. Giaccia, Hypoxia-mediated selection of cells with diminished apoptotic potential in solid tumours, Nature, 379 (1996), 88–91.
[48] H. P. Greenspan, Models for the growth of a solid tumor by diffusion, Stud. Appl. Math., 52 (1972), 317–340.
[49] ———, On the growth and stability of cell cultures and solid tumors, J. Theor. Biol., 56 (1976), 229–242.

[50] W. C. Hahn and R. A. Weinberg, Modelling the molecular circuitry of cancer, Nature Rev., 2 (2002), 331–341.
[51] D. Hanahan and R. A. Weinberg, The hallmarks of cancer, Cell, 100 (2000), 57–70.
[52] H. W. Hann, M. W. Stahlhut, and C. L. Hann, Effect of iron and desferoxamine on cell growth and *in vitro* ferritin synthesis in human hepatoma cell lines, Hepatology, 11 (1990), 566–569.
[53] S. W. Hayward, Y. Wang, M. Cao, Y. K. Hom, B. Zhang, G. D. Grossfeld, D. Sudilovski, and G. R. Cunha, Malignant transformation in a nontumorigenic human prostatic epithelial cell line, Cancer Res., 61 (2001), 8135–8142.
[54] S. Hellman, Principles of cancer managemant: Radiation therapy, in Cancer: Principles and Practice of Oncology, V. T. DeVita, S. Hellman, and S. A. Rosenberg, eds., Lippencott-Raven, Philadelphia, 5th ed., 1997, ch. 16, 307–332.
[55] G. Helmlinger, P. A. Netti, H. C. Lichtenbeld, R. J. Melder, and R. K. Jain, Solid stress inhibits the growth of multicellular tumor spheroids, Nature Biotech., 5 (1997), 778–783.
[56] M. W. Hirsch, S. Smale, and R. L. Devaney, Differential Equations, Dynamical Systems, and an Introduction to Chaos, Elsevier, Amsterdam, 2nd ed., 2004.
[57] J. Holash, P. C. Maisonpierre, D. Compton, P. Boland, C. R. Alexander, D. Zagzag, G. D. Yancopolous, and S. J. Weigand, Vessel cooperation, regression and growth in tumors mediated by angiopoietins and VEGF, Science, 221 (1998), 1994–1998.
[58] D. E. Ingber, Cancer as a disease of epithelial-mesenchymal interactions and extracellular matrix regulation, Differentiation, 70 (2002), 547–560.
[59] R. K. Jain, Normalization of tumor vasculature: An emerging concept in antiangiogenic therapy, Science, 307 (2005), 58–62.
[60] Y. Kuang, J. D. Nagy, and J. J. Elser, Biological stoichiometry of tumor dynamics: Mathematical models and analysis, Disc. Cont. Dyn. Sys. B, 4 (2004), 221–240.
[61] L. A. Kunz-Schughart, Multicell tumor spheroids: Intermediates between monolayer culture and *in vivo* tumor, Cell Biol. Int., 23 (1999), 157–161.
[62] K. Landman and C. P. Please, Tumor dynamics and necrosis: Surface tension and stability, IMA J. Math. Appl. Med. Biol., 18 (2001), 131–158.
[63] N. T. Le and D. R. Richardson, The role of iron in cell cycle progression and the proliferation of neoplastic cells, Biochim. Biophys. Acta, 1603 (2002), 31–46.
[64] S. C. Lester and R. S. Cotran, The breast, in Robbins' Pathologic Basis of Disease, R. S. Cotran, V. Kumar, and T. Collins, eds., W. B. Saunders, Philadelphia, 6th ed., 1999, ch. 25, 1093–1119.
[65] H. A. Levine, S. Pamuk, B. D. Sleeman, and M. Nilsen-Hamilton, Mathematical modeling of capillary formation and development in tumor angiogenesis: Penetration into the stroma, Bull. Math. Biol., 63 (2001), 801–863.
[66] H. A. Levine and B. D. Sleeman, Modelling tumor-induced angiogenesis, in Cancer Modelling and Simulation, L. Preziosi, ed., Chapman and Hall/CRC, Boca Raton, FL., 2003.
[67] L. A. Liotta and E. C. Kohn, The microenvironment of the tumour-host interface, Nature, 411 (2001), 375–379.
[68] L. A. Loeb, A mutator phenotype in cancer, Cancer Res., 61 (2001), 3230–3239.
[69] L. A. Loeb, K. R. Loeb, and J. P. Anderson, Multiple mutations and cancer, Proc. Natl. Acad. Sci. USA, 100 (2003), 776–781.
[70] A. S. Lundberg and R. A. Weinberg, Control of the cell cycle and apoptosis, Eur. J. Cancer, 35 (1999), 1886–1894.
[71] C. C. Lynch and L. M. Matrisian, Matrix metalloproteinases in tumor-host cell communication, Differentiation, 70 (2002), 561–573.
[72] N. V. Mantzaris, S. Webb, and H. G. Othmer, Mathematical modeling of tumor-induced angiogenesis, J. Math. Biol., 49 (2004), 111–187.
[73] J. Maynard Smith and G. R. Price, Logic of animal conflict, Nature, 246 (1973), 15–18.
[74] S. Michelson and J. T. Leith, Positive feedback and angiogenesis in tumor growth control, Bull. Math. Biol., 59 (1997), 233–254.
[75] S. Michelson, B. E. Miller, A. S. Glicksman, and J. T. Leith, Tumor micro-ecology and competitive interactions, J. Theor. Biol., 128 (1987), 233–246.

[76] F. Mollica, R. K. Jain, and P. A. Netti, A model for temporal heterogeneities of tumor blood flow, Microvasc. Res., 65 (2003), 56–60.
[77] W. Mueller-Klieser, Three-dimensional cell cultures: From molecular mechanisms to clinical applications, Am. J. Physiol., 273 (1997), C1109–C1123.
[78] ———, Tumor biology and experimental therapeutics, Crit. Rev. Oncol. Hematol., 36 (2000), 123–139.
[79] B. J. Murphy, Regulation of malignant progression by the hypoxia-sensitive transcription factors HIF-1α and MTF-1, Comp. Biochem. Physiol. B, 139 (2004), 495–507.
[80] J. D. Murray, Mathematical Biology I: An Introduction, Springer-Verlag, Berlin, 2nd ed., 2002.
[81] ———, Mathematical Biology II: Spatial Models and Biomedical Applications, Springer-Verlag, Berlin, 2nd ed., 2002.
[82] J. D. Nagy, Competition and natural selection in a mathematical model of cancer, Bull. Math. Biol., 66 (2004), 663–687.
[83] P. C. Nowell, The clonal evolution of tumor cell populations, Science, 194 (1976), 23–28.
[84] L. Nunney, Lineage selection and the evolution of multistage carcinogenesis, Proc. R. Soc. Lond. B, 266 (1999), 493–498.
[85] K. Ohuchida, K. Mizumoto, M. Murakami, L.-W. Qian, N. Sato, E. Nagai, K. Matsumoto, T. Nakamura, and M. Tanaka, Radiation to stromal fibroblasts increases invasiveness of pancreatic cancer cells through tumour-stromal interactions, Cancer Res., 64 (2004), 3215–3222.
[86] A. F. Olumi, G. D. Grossfeld, S. W. Hayward, P. R. Carroll, T. D. Tlsty, and G. R. Cunha, Carcinoma-associated fibroblasts direct tumour progression of initiated human prostatic epithelium, Cancer Res., 59 (1999), 5002–5011.
[87] S. Ono, Genetic implication of karyological instability of malignant somatic cells, Physiol. Rev., 51 (1971), 496–526.
[88] M. R. Owen and J. A. Sherratt, Mathematical modelling of macrophage dynamics in tumours, Math. Mod. Methods Appl. Sci., 9 (1999), 513–539.
[89] C. C. Park, M. J. Bissel, and H. Barcellos-Hoff, The influence of the microenvironment on the malignant phenotype, Mol. Med. Today, 6 (2000), 324–329.
[90] A. A. Patel, E. T. Gawlinski, S. K. Lemieux, and R. A. Gatenby, A cellular automaton model of early tumor growth and invasion: The effects of native tissue vascularity and increased anaerobic tumor metabolism, J. Theor. Biol., 213 (2001), 315–331.
[91] G. P. Pescramona, M. Scalerano, P. P. Delsanto, and C. A. Condat, Non-linear model of cancer growth and metastasis: A limiting nutrient as a major determinant of tumor shape and diffusion, Med. Hypotheses, 53 (1999), 497–503.
[92] M. J. Plank and B. D. Sleeman, Lattice and non-latice models of tumour angiogenesis, J. Math. Biol., 66 (2004), 1785–1819.
[93] C. P. Please, G. Pettet, and D. L. S. McElwain, A new approach to modelling the formation of necrotic regions in tumours, Appl. Math. Lett., 11 (1998), 89–94.
[94] ———, Avascular tumour dynamics and necrosis, Math. Mod. Meth. Appl. Sci., 9 (1999), 569–579.
[95] B. A. J. Ponder, Cancer genetics, Nature, 411 (2001), 336–341.
[96] V. Quaranta, Motility cues in the tumor microenvironment, Differentiation, 70 (2002), 590–598.
[97] N. Raghunand, R. A. Gatenby, and R. J. Gillies, Microenvironmental and cellular consequences of altered blood flow in tumours, Br. J. Radiol., 76 (2003), 11–22.
[98] C. D. Roskelley and M. J. Bissel, The dominance of the microenvironment in breast and ovarian cancer, Cancer Biol., 12 (2002), 97–104.
[99] J. A. Royds, S. K. Downer, E. E. Qwarnstrom, and C. E. Lewis, Responses of tumour cells to hypoxia: Role of p53 and NFκB, Mol. Pathol., 51 (1998), 55–61.
[100] T. Shiomi and Y. Okada, MT1-MMP and MMP-7 in invasion and metastasis of human cancers, Cancer Metastasis Rev., 22 (2003), 145–152.
[101] R. W. Sterner and J. J. Elser, Ecological Stoichiometry: The Biology of Elements from Molecules to the Biosphere, Princeton University Press, Princeton, NJ, 2002.

[102] B. R. Stoll, C. Migliorini, A. Kadambi, L. L. Munn, and R. K. Jain, A mathematical model of the contribution of endothelial progenitor cells to angiogenesis in tumors: Implications for antiangiogenic therapy, Blood, 102 (2003), 2555–2561.
[103] B. Subramanian and D. E. Axelrod, Progression of heterogeneous breast tumors, J. Theor. Biol., 210 (2001), 107–119.
[104] R. M. Sutherland, Importance of critical metabolites and cellular interactions in the biology of microregions of tumors, Cancer, 58 (1986), 1668–1680.
[105] R. M. Sutherland, J. A. McCredie, and W. R. Inch, Growth of multicell spheroids in tissue culture as a model of nodular carcinomas, J. Natl. Cancer Inst., 46 (1971), 113–120.
[106] K. E. Thompson and J. A. Royds, Hypoxia and reoxygenation: A pressure for mutant p53 cell selection and tumor progression, Bull. Math. Biol., 61 (1999), 759–778.
[107] S. Tohya, A. Mochizuki, S. Imayama, and Y. Iwasa, On rugged shape of skin tumor (basal cell carcinoma), J. Theor. Biol., 194 (1998), 65–78.
[108] I. P. Tomlinson and W. F. Bodmer, Modelling the consequences of interactions between tumour cells, Br. J. Cancer, 75 (1997), 157–160.
[109] I. P. M. Tomlinson, Game-theory models in interactions between tumor cells, Eur. J. Cancer, 33 (1997), 1495–1500.
[110] R. H. Tomlinson and L. H. Gray, The histological structure of some human lung cancers and possible implications for radiotherapy, British Journal of Cancer, 9 (1955), 539–549.
[111] M. E. Valk-Lingbeek, S. W. M. Bruggeman, and M. van Lohuizen, Stem cells and cancer: The polycomb connection, Cell, 118 (2004), 409–418.
[112] B. Vogelstein, E. R. Fearon, S. R. Hamilton, A. C. Preisinger, H. F. Willard, A. M. Michelson, and S. H. Orkin, Clonal analysis using recombinant DNA probes from the X-chromosome, Cancer Res., 47 (1987), 4806–4813.
[113] R. A. Weinberg, One Renegade Cell, Basic Books, New York, 1998.
[114] N. Wernert, The multiple roles of tumour stroma, Virchows Arch., 430 (1997), 433–443.
[115] N. Wernert, C. Löcherbach, A. Wellman, P. Behrens, and A. Hügel, Presence of genetic alterations in microdissected stroma of human colon and breast cancers, Anticancer Res., 21 (2001), 2259–2264.
[116] G. N. Wogan, S. S. Hecht, J. S. Felton, A. H. Conney, and L. A. Loeb, Environmental and chemical carcinogenesis, Sem. Cancer Biol., 14 (2004), 473–486.
[117] Y. Xu, A free boundary problem model of ductal carcinoma *in situ*, Disc. Cont. Dyn. Sys. B, 4 (2004), 337–348.

Received on January 15, 2005. Revised on March 11, 2005.

E-mail address: john.nagy@sccmail.maricopa.edu